Plastic instability of platinum modified and unmodified aluminide coatings during 1100 C cyclic testing

McCloskey, Margaret Ann

Monterey, California: U.S. Naval Postgraduate School

NAVAL POSTGRADUATE SCHOOL
Monterey, California

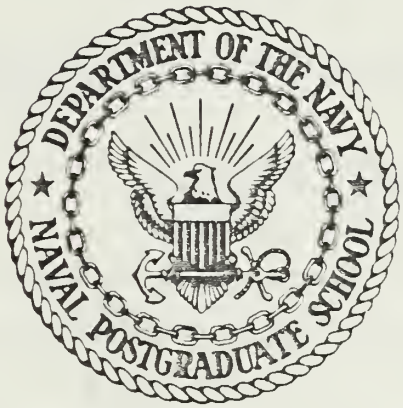

THESIS

PLASTIC INSTABILITY OF PLATINUM MODIFIED AND
UNMODIFIED ALUMINIDE COATINGS
DURING 1100 C CYCLIC TESTING

by

Margaret Ann McCloskey

September 1986

Thesis Advisor: D.H. Boone

SECURITY CLASSIFICATION OF THIS PAGE

REPORT DOCUMENTATION PAGE

1a REPORT SECURITY CLASSIFICATION UNCLASSIFIED	1b RESTRICTIVE MARKINGS
2a SECURITY CLASSIFICATION AUTHORITY	3 DISTRIBUTION / AVAILABILITY OF REPORT Approved for public release; distribution is unlimited
2b DECLASSIFICATION / DOWNGRADING SCHEDULE	
4 PERFORMING ORGANIZATION REPORT NUMBER(S)	5 MONITORING ORGANIZATION REPORT NUMBER(S)
6a NAME OF PERFORMING ORGANIZATION Naval Postgraduate School 6b OFFICE SYMBOL (If applicable) 69	7a NAME OF MONITORING ORGANIZATION Naval Postgraduate School
6c ADDRESS (City, State, and ZIP Code) Monterey, California 93943-5100	7b ADDRESS (City, State, and ZIP Code) Monterey, California 93943-5100
8a NAME OF FUNDING / SPONSORING ORGANIZATION 8b OFFICE SYMBOL (If applicable)	9 PROCUREMENT INSTRUMENT IDENTIFICATION NUMBER
8c ADDRESS (City, State, and ZIP Code)	10 SOURCE OF FUNDING NUMBERS PROGRAM ELEMENT NO / PROJECT NO / TASK NO / WORK UNIT ACCESSION NO

11 TITLE (Include Security Classification)
PLASTIC INSTABILITY OF PLATINUM MODIFIED AND UNMODIFIED ALUMINIDE COATINGS DURING 1100 C CYCLIC TESTING

12 PERSONAL AUTHOR(S)
McCloskey, Margaret Ann

13a TYPE OF REPORT	13b TIME COVERED	14 DATE OF REPORT (Year, Month, Day)	15 PAGE COUNT
Master's Thesis	FROM _____ TO _____	1986 September	61

16 SUPPLEMENTARY NOTATION

17 COSATI CODES			18 SUBJECT TERMS (Continue on reverse if necessary and identify by block number)
FIELD	GROUP	SUB-GROUP	Turbine Blade Coatings; Platinum-Aluminides; Diffusion Coatings; IN-738; Coating Plastic Instability; Rumpling

19 ABSTRACT (Continue on reverse if necessary and identify by block number)

In a study conducted at the Naval Postgraduate School on the effect of cyclic oxidation at 1100 C on platinum modified and unmodified aluminide coated nickel base superalloy (IN-738), a surface deformation described as rumpling was first reported. Rumpling was found to be a function of the number and type of thermal strain cycles, thermal expansion mismatch, coating strength and coating thickness. Further testing to determine the mechanical and protectivity impact of rumpling has been conducted. In addition, a concurrent study of the beta(NiAl) phase degradation was undertaken.

20 DISTRIBUTION / AVAILABILITY OF ABSTRACT	21 ABSTRACT SECURITY CLASSIFICATION
☒ UNCLASSIFIED/UNLIMITED ☐ SAME AS RPT ☐ DTIC USERS	UNCLASSIFIED
22a NAME OF RESPONSIBLE INDIVIDUAL D.H. Boone	22b TELEPHONE (Include Area Code) (408) 646-2551 22c OFFICE SYMBOL 69Bl

DD FORM 1473, 84 MAR 83 APR edition may be used until exhausted
All other editions are obsolete

SECURITY CLASSIFICATION OF THIS PAGE

Approved for public release; distribution is unlimited.

Plastic Instability of Platinum Modified and Unmodified Aluminide Coatings During 1100 C Cyclic Testing

by

Margaret Ann McCloskey
Lieutenant, United States Navy
B.S., Belmont Abbey College, 1977

Submitted in partial fulfillment of the
requirements for the degree of

MASTER OF SCIENCE IN MECHANICAL ENGINEERING

from the

NAVAL POSTGRADUATE SCHOOL
September 1986

ABSTRACT

In a study conducted at the Naval Postgraduate School on the effect of cyclic oxidation at 1100 C on platinum modified and unmodified aluminide coated nickel base superalloy (IN-738), a surface deformation described as rumpling was first reported. Rumpling was found to be a function of the number and type of thermal strain cycles, thermal expansion mismatch, coating strength and coating thickness. Further testing to determine the mechanical and protectivity impact of rumpling has been conducted. In addition, a concurrent study of the β(NiAl) phase degradation was undertaken.

TABLE OF CONTENTS

I. INTRODUCTION 8

II. BACKGROUND 10

A. HIGH TEMPERATURE OXIDATION AND HOT CORROSION 10

B. DIFFUSION ALUMINIDE COATINGS 13

C. PLATINUM MODIFIED ALUMINIDES 15

D. RUMPLING 16

III. EXPERIMENTAL PROCEDURES 19

A. APPARATUS 19

B. SPECIMEN PREPARATION 19

C. EXPERIMENTAL TESTING 20

D. DATA ANALYSIS 20

IV. RESULTS AND DISCUSSION 21

A. GENERAL OBSERVATIONS 21

B. RUMPLING 21

C. MICROSTRUCTURAL CHANGES 24

V. CONCLUSIONS 26

APPENDIX A: TABLES 27

APPENDIX B: FIGURES 31

LIST OF REFERENCES 57

INITIAL DISTRIBUTION LIST 60

LIST OF TABLES

I. OXIDE-METAL VOLUME RATIOS 27

II. 738 IN-738 COMPOSITION (WEIGHT PERCENT) 28

III. NPS STANDARD PRE-ALUMINIZING HEAT TREATMENTS* 28

IV. CODING SYSTEM FOR PLATINUM ALUMINDE AND ALUMINIDE COATINGS 29

V. SPECIMEN LISTING 29

VI. CYCLIC EXPOSURE LINEAL ROUGHNESS DATA 30

LIST OF FIGURES

B.1 Lineal Surface Roughness Measurement 31

B.2 Horizontal Cyclic Oxidation Rig and Associated Thermal Cycle 32

B.3 Rumpled Baseline and Platinum Aluminide Specimen Surfaces, 275 Cycles (32 ×): a) BLA, b) 1IIAt, c) 2IIAt, d) 3IIAt 33

B.4 Rumpled Platinum Aluminide Specimen Surfaces, 275 Cycles, (32 ×): a) 1IIBT, b) 2IIBT, c) 3IIBT, d) 4IIBT 34

B.5 Rumpling During Thermal Cycling for the Platinum Aluminide Coating 3IIBt, (250 ×): a) 0 cycles, b) 150 cycles, c) 275 cycles 35

B.6 Rumpling During Thermal Cycling for the Platinum Aluminide Coating 4IIBT, (250 ×): a) 0 cycles, b) 150 cycles, c) 275 cycles 36

B.7 Rumpling During Thermal Cycling for the Inward Baseline Coating BLA, (250 ×): a) 0 cycles, b) 150 cycles, c) 275 cycles 37

B.8 Rumpling During Thermal Cycling for the Outward Baseline Coating BLB, (250 ×): a) 0 cylces, b) 150 Cycles, c) 275 cycles 38

B.9 Plot of Lineal Roughness versus Cyclic Exposure for Thin Inward Platinum Aluminide Coating and Baseline Specimens 39

B.10 Plot of Lineal Roughness versus Cyclic Exposure for Thin Outward Platimum Aluminide Coating and Baseline Specimens 40

B.11 Rumpling Comparison of Thin Inward Platinum Aluminide Coatings 275 Cycled, (250 ×): a) 1IIAt, b) 2IIAt, c) 3IIAt 41

B.12 Rumpling Comparison of Thin Outward Platinum Aluminide Coatings 275 Cycles, (250 ×): a) 1IIBt, b) 3IIBt 42

B.13 Plot of Lineal Roughness versus Cyclic Exposure for Thick Outward Platinum Aluminide Coating Specimens 43

B.14 Rumpling Comparisons of Thick Outward Platinum Aluminide Coatings 275 Cycles, (250 ×): a) 2IIBT, b) 3IIBT, c) 4IIBT 44

B.15 Rumpling Comparisons of Thick Inward Platinum Aluminide Coatings 275 Cycles, (250 ×): a) 3IIAT, b) 4IIAT 45

B.16 Thickness Rumpling Effect for Similarly Processed Platinum Aluminide Coatings, 275 Cycles, (250 ×): a) 1IIBt, b) 1IIBT, ... 46

B.17 Plot of Lineal Roughness versus Cyclic Exposure for a Thin and Thick Inward and Outward Platinum Aluminide Coating 47

B.18 Rumpling Comparison of a Thin and Thick Platinum Aluminide Coating, 150 Cycles, (250 ×): a) 3IIBT, b) 3IIBt 48

B.19 Plot of Lineal Roughness versus Cyclic Exposure for Smooth and Rough Platinum Aluminide Coatings 49

B.20 Rumpling Comparisons of a Smooth and Rough Platinum Aluminide Coating, (250 ×): a) RIIC, 150 cycles, b) SIIC, 150 cycles, c) RIIC, 275 cycles, d) SIIC, 275 cycles 50

B.21 Cross-section Microstructural Comparison of Initial and Thermally Cycled Platinum Aluminide Coatings, (650 ×): a) 2IIAt, 0 cylces, b) 2IIAt, 150 cycles, c) 3IIAt, 0 cycles, d) 3IIAt, 150 cycles 51

B.22 Cross-section Microstructural Comparison of An Initial and Thermally Cycled Platinum Aluminide Coating, (650 ×): a) 4IIAT, 0 cycles, b) 4IIAT, 150 cycles 52

B.23 Cross-section Microstructural Comparison of An Initial and Thermally Cycled Platinum Aluminide Coating, (650 ×): a) 4IIBT, 0 cycles, b) 4IIBT, 150 cycles 53

B.24 Cross-section Microstructural Comparison of the Inward Baseline Coating, Initial and Thermally Cycled: a) BLA, 0 cycles (650 ×), b) BLA, 150 cycles (550 ×), c) BLA, 275 cycles (500 ×) 54

B.25 Cross-section Microstructural Comparison of the Outward Baseline Coating, Initial and Thermally Cycled: a) BLB, 0 cycles (550 ×), b) BLB, 150 cycles (550 ×), c) BLB, 275 cycles (500 ×) 55

B.26 Cross-section Microstructural Comparison of a Platinum Aluminide Coating, Initial and Thermally Cycled: a) 3IIBt, 0 cycles (500 ×), b) 3IIBt, 150 cycles (650 ×), c) 3IIBt, 275 cycles (500 ×) 56

I. INTRODUCTION

Gas turbines have increasingly become the choice by industry and the military for use in power generation and propulsion plants. The many advantages of gas turbine propulsion systems have led the United States Navy to adopt them for use in several marine vehicles, including the DD-963 class destroyers, the CG-47 class cruisers, the FFG-7 class frigates and the PHM class gunboats.

Continued development of the gas turbine propulsion system has led to production of high temperature resistant superalloys to meet the high performance and cost-effectiveness requirements of the gas turbine engine. These superalloys have been designed to enhance bulk mechanical properties such as high temperature creep rupture strength, fatigue life and castability [Ref. 1:p. 165]. Simultaneously however, the superalloys' resistance to corrosion was decreased. Higher turbine inlet temperatures and thinner blade walls necessary for internal cooling systems also contribute to the reduction of engine life as a result of premature surface degradation. In addition and probably of most importance, the marine enviroment aggressively contributes to metallic corrosion and oxidation by virtue of the contaminants such as sulfur and salts that are contained in the fuel and air.

Avenues leading to improvements in longer engine life in the marine enviroment are limited. Seeking to improve the quality of fuel so as to avoid hot corrosion of the turbine components is unfeasible: initially the cost of such fuels would be prohibitive; projected supply inadequacies in wartime finalize the question of improved fuel. In order not to sacrifice overall system performance by lowering design specifications, the most logical approach to improving engine life, specifically turbine blade life, has been to provide additional protection to the turbine components in the form of coatings, i.e. the use of a composite system.

The objective of a coating is to offer increased protection against high temperature oxidation and hot corrosion without degrading the mechanical properties of its substrate. This provides an increased component life while sustaining its high performance, thereby raising the efficiency and lowering the total cost of the gas turbine by increasing its time between overhauls. For use in high temperature enviroments, the common design goal for coatings is to form an adherent, protective scale of aluminum oxide in simple oxidation.

For the past few decades aluminide diffusion coatings have been the primary method used to achieve this result. But as improved performance designs for gas turbines raised the operating temperature, the aluminide diffusion coatings have increasingly become inadequate as a means of total protection. To extend the life of the coating to be compatible with the component life, it was found that the addition of noble elements to the aluminide coating system enhanced the adhesion of the protective oxide scale and apparently the mechanical properties of the scale. Platinum was one such addition; the platinum modified aluminide coatings have undergone a great deal of research and development as one of the more viable options. Contributing to these efforts have been the ongoing studies at the Naval Postgraduate School, Department of Mechanical Engineering.

The objectives of this thesis are two-fold: 1) to further investigate the degradation of the platinum modified aluminide coatings during cyclic oxidation; and 2) to continue a study on surface plastic instability, so called "rumpling", of the coatings.

II. BACKGROUND

A. HIGH TEMPERATURE OXIDATION AND HOT CORROSION

Corrosion processes describe the detrimental alloy-enviroment interactions occuring in nearly all engineering applications of metallic alloys. These interactions result in the alloy surfaces undergoing compositional and phase changes, leaving a surface that is not as effective as the alloy in performing the specified engineering function [Ref. 2:p. 603]. The two most degrading forms of corrosion for gas turbines are high temperature oxidation and hot corrosion.

Oxidation is a reaction that takes place upon exposure of the metal to a source of oxygen when the oxygen pressure is greater than that required for the metal--metal oxide equilibrium [Ref. 2:p. 604]. This conversion of metal to metal oxide can quickly become critical in components that are thin by design; specifically, unchecked oxide penetration reduces the effective cross-sectional area, thereby reducing the component's load-carrying capacity [Ref. 3:p. 145], and close tolerance requirements can be interfered with by the build up of the oxide. Since the equilibrium oxygen pressures for most metals are very small, the thermodynamic conditions are favorable for oxide formation in many gas enviroments. The effect of elevated temperatures upon oxide scale formation on metals is demonstrated by the relationship

$$(PO)^{1/2}_{M\text{-}MO} = \exp(+\Delta G^{0}_{MO} RT) \qquad \text{(eqn 2.1)}$$

where $(PO)_{M\text{-}MO}$ is the oxygen pressure of the metal--metal oxide equilibrium, T is the absolute temperature and ΔG^{0}_{MO} is the standard free energy of formation of the oxide MO [Ref. 2:p. 604]. If the scale formed is dense and protective, the oxidation rate decreases with time: oxidation is inhibited as the scale acts as a barrier between the metal and oxygen, reducing the diffusion of the oxygen and/or metal ions thus slowing the oxidation reaction. If, on the other hand, a porous and/or nonadherent scale is formed, the oxidation reaction generally leads to such a destruction of the alloy surface that component failure occurs.

In an alloy exposed to oxygen, oxides of all the reactive elements in the alloy will be formed, the film consisting of the oxides in proportion to the alloy composition

[Ref. 4:p. 14]. This is referred to as the transient or initial stage. During this stage the oxides are in competition with each other; the oxide with the greatest thermodynamic stability eventually dominates. This then forms a continuous surface layer, its kinetics of formation favoring lateral growth being one of the factors in its dominance [Ref. 2:p. 608]. It is by controlling this selective oxidation that a protective coating may be formed vice an unprotective one.

In light of this process of selective oxidation, one problem with nickel base alloys can be overcome. Nickel oxide (NiO) is a metal-deficient oxide: two trivalent nickel ions exist for each nickel ion vacancy in normal lattice positions [Ref. 5:p. 511]. This affects the diffusion of ionic defects through the scale, which is the controlling factor in this oxidation. To increase, then, the oxidation rate of nickel alloys toward providing a protective scale, chromium is added to the alloy. Generally a few percent of chromium is required, the oxidation rate increasing up to about 5% chromium [Ref. 5:p. 518], the protective oxide phase Cr_2O_3 being formed. Since the alloy will become depleted of the chromium due to its selective oxidation, a chromium content high enough to ensure a continuous protective layer over the surface layer of the alloy must be incorporated into the alloy's composition.

However, "chromium scales cannot be used at temperatures above about 1000 C as gaseous CrO_3 is formed which causes its protectiveness to be decreased." [Ref. 2:p. 609] To circumvent this complication, and in conjunction with its addition for strengthening, aluminum is added to the nickel alloy, as it forms a protective oxide phase α-Al_2O_3 which is thermodynamically stable [Ref. 5:p. 524]. In addition the presence of chromium allows aluminum to be selectively oxidized at lower aluminum concentrations [Ref. 2:p. 610].

There are several characteristics that an oxide must possess to be protective: good adherence, a high melting point, a low vapor pressure, good high-temperature plasticity to resist fracture and low electrical conductivity or low diffusion coefficients for metal ions and oxygen [Ref. 5:p. 506]. (In addition, the metal and oxide should have similar coefficients of expansion for cyclic temperature operation.) Pilling and Bedworth [Ref. 6] proposed that the volume ratio of oxide and metal per gm atom of metal would indicate the oxidation resistance of an oxide. The ideal ratio would be close to unity; less than that results in insufficient oxide to cover the metal and a ratio much greater than 1 tends to introduce large compressive stresses in the oxide. (The latter causes poor oxidation resistance due to cracking and spalling.) Table 1 [Ref. 7:p. 445] illustrates the relative superiority of chromium and aluminum oxides.

Hot corrosion is defined as deposit modified, gas-induced degradation of alloys [Ref. 2:p. 619], and or an accelerated oxidation attack due to the presence of alkali metal salts [Ref. 4:p. 46]. Although there is not complete agreement as to the mechanisms of hot corrosion, it has been widely accepted [Refs. 2,4,8,9] that the protective scale becomes porous and non-adherent due to fluxing (dissolution) by the molten salts. This reaction of the oxide scales with the liquid deposit is classified in one of two ways: if occuring through reaction with oxide ions in the deposit, the reactions are said to be basic, while they are termed acidic when oxide ions are donated to the deposit by the oxide scale [Ref. 2:p. 620].

Attack by hot corrosion can be briefly described in two steps, generally referred to as the initiation stage and the propagation stage. Fluxing of the surface oxides into a molten state by the metal salts degrades the desired protective oxide. The salt is then able to penetrate the oxide to react directly with the base metal. The base metal is aggressively attacked as it is usually depleted of the protective alloying elements (from previous formation of the protective oxides), and oxide reformation is prevented. Rapid deterioration of the base metal follows. [Ref. 10:p. 1] In gas turbines operating in a marine enviroment, Na_2SO_4 (Na^- ingested with the air and Na^- and S^- from fuels) plays a major role in hot corrosion attack, with the corrosion rate being proportional to the sulfur content of the fuel since it is proportional to the partial pressure of SO_3 [Ref. 11:p. 8].

Factors affecting hot corrosion include temperature and frequency of thermal cycling. Hot corrosion does not occur below the eutectic melting temperature of the salt (at the process pressure) nor above the boiling temperature [Ref. 5:p. 541], with the maximum attack occuring at an intermediate temperature. In the seventies it was recognized for the first time that there were two distinct classifications of hot corrosion, low temperature hot corrosion (LTHC) and high temperature hot corrosion (HTHC), occuring in the temperature ranges 600-700 C and 800-1000 C, respectively [Ref. 8:p. 66]. Low temperature hot corrosion is equivalent to acidic fluxing, while basic fluxing occurs at high temperatures [Ref. 11:p. 6]. Microstructurally the degradations are different, with Shepard [Ref. 8:p. 66] characterizing LTHC as a "pitting" type of attack with no depletion zone, with HTHC causing significant alloy depletion zone.[1]

[1]These descriptions refer to hot corrosion of aluminide coatings and nickel base alloys.

Thermal cycling accelerates the transition from the initiation stage of hot corrosion to the propagation stage [Ref. 12:p. 6]. During the first stage the reaction product barrier that forms due to reaction of the alloy with the gas is developing beneath the salt deposit. This product can crack and spall due to thermal cycling. The cyclic thermal strains are caused by coating--superalloy mechanical incompatibility: different coefficients of thermal expansion lead to the development of significant mismatch strains [Ref. 12:p. 25]. A tensile thermal expansion mismatch strain increases the coating strain, leading to cracking. Thus thermal cycling shortens the transition time from the initiation stage to the propagation stage of hot corrosion.

Nickel base alloys are susceptible to basic fluxing. To combat this, the chromium content is increased. At higher chromium concentrations, continuous Cr_2O_3 scales are formed which are less susceptible to solution and repreciptation from the Na_2SO_4. An increased chromium concentration also inhibits degradation via sulfidation, another form of hot corrosion which occurs after initial surface breakdown; the chromium combines with the sulfur to form sulfides which have higher melting points. Varying concentration levels are cited as the minimum levels, from 15-20% [Ref. 4:p. 47] to 18 or more percent [Ref. 8:p. 74]. However, chromium concentrations higher than 15-20% interfere with the gamma prime $\{Ni_3(Al,Ti)\}$ phase that nickel base alloys use for precipitation hardening [Ref. 5:p. 521] by promoting the titanium in the alloy to form embrittling TCP phases [Ref. 3:p. 145]. In most cases the composition of a superalloy is a compromise between high-temperature oxidation/hot corrosion resistance and high-temperature strength.

B. DIFFUSION ALUMINIDE COATINGS

The development of high-temperature superalloys with increased strength and other improved mechanical properties has not coincided with retention of the surface stability of the alloys; instead, the superalloys have demonstrated a reduction in high temperature oxidation and hot corrosion resistance, in part due to the decrease in chromium content nesessary for high temperature strength requirements. To provide the superalloys with both characteristics, a "composite-system" utilizing coatings on strong base metals [Ref. 3:p. 143] was first employed in the sixties. The ability to form alumina (Al_2O_3) or chromia (Cr_2O_3) scales was the factor in selecting specific coating compositions. For nickel base superalloys, nickel aluminide, β(NiAl), is the optimum coating compound [Ref. 13:p. 676], aluminum is the only element possessing the

required primary properties of formation of an oxide with low transport rates and a relative degree of high-temperature compatability with nickel base superalloys [Refs. 2,11:p. 633, 3]. Hence, diffusion aluminide coatings have been most commonly used.

Diffusion coatings, by their nature, form a metallurgical band with the base metal. This diffusion interaction between the coating constituents and the substrate can lower the substrate's tensile, creep and fatigue properties, yet ductile coatings can increase the thermal fatigue properties [Ref. 12:p. 3]. To restore mechanical properties, postcoating heat treatments are used [Refs. 3,14:p. 165, 208].

Pack cementation processes have been the method of choice for application of the diffusion aluminide coatings. These processes have been described in detail elsewhere [Refs. 3,13:pp. 148-149, 677-678]. Two structural types are obtained, depending on the aluminum activity, which determines the nickel-aluminum intermetallic phase formed on the alloy surface. High activity processes at low temperatures (LTHA) produce a Ni_2Al_3 phase resulting in inward diffusion of aluminum, while outward diffusion of nickel in nickel-rich NiAl is derived from low activity processes at high temperatures (HTLA) [Ref. 2:p. 630]. It has been determined that the most desirable phase an intermediate aluminum content (24-30%) β-NiAl [Ref. 3:p. 147], its stability determines the protective qualities of the coating.

The protection provided by diffusion aluminide coatings is based on their ability to form and replenish alumina scales. In addition to design considerations, as when used with thin-walled components, increasing coating thickness to provide for a larger reservoir of aluminum results in a decrease in ductility, further resulting in cracking and spalling of the coating [Ref. 13:p. 677]. Furthermore, the alumina scales characteristically adhere poorly to the underlying coating alloy and are therefore prone to spall under cyclic oxidation conditions [Refs. 15,16,17]. Continual spalling of the alumina scales due to thermal stresses and erosion induced by high velocity gases, and subsequent replenishment of the oxide serve to deplete the aluminum concentration in the coating. While the diffusion aluminde coatings have been found to have good resistance to oxidation up to about 980 C [Ref. 3:p. 147], degradation due to interdiffusion is sometimes found at higher temperatures. Diffusion of the aluminum out of the coating or of substrate elements into the coating, further decreasing the coating aluminum concentration, degrades the coating's resistance to high-temperature hot corrosion [Ref. 18:p. A2].

C. PLATINUM MODIFIED ALUMINIDES

With improved gas turbine designs and again better superalloys, diffusion aluminide coatings became inadequate in performance in the increasingly high temperature, corrosive marine enviroment. In hopes of creating a more effective diffusion barrier for the aluminum, platinum was added to the superalloy surface before the aluminizing process It was found, however, that instead of acting as a diffusion barrier, the platinum was concentrated towards the outer surface of the coating, yet the platinum-modified aluminide coating demonstrated a significantly improved resistance to high temperature corrosion. Lehnert and Meinhardt's publications [Ref. 19,20] stimulated numerous studies on the effects of platinum on the oxidation resistance of alloy systems that form external scales of α-Al_2O_3.[2] These and other works culminated in several commercially available, platinum modified aluminide coatings. It was generally concluded that the coatings provided both enhanced high temperature oxidation resistance and hot corrosion resistance under basic fluxing conditions, but offered little or no improvement in resistance to hot corrosion under acidic conditions [Ref. 11:p. 11].

In a recent review of the corrosion behavior of platinum modified aluminde coatings by Deb and Boone [Ref. 9:p. 8] it was concluded that the protectivity performance of the coatings is "strongly dependent on structure and composition". Additionally, a preliminary investigation [Ref. 21:p. 12] showed that a structural dependence for oxidation resistance may also exist. A knowledge of the microstructures of the various platinum modified aluminide coatings is therefore essential for the understanding of the protection offered by them. Several factors shape the microstructural features including the initial thickness of platinum, the pre-aluminizing diffusion treatments the conditions used in the pack-cementation aluminizing process and the post-aluminizing heat treatment [Refs. 9,18:pp. 12, A5-A6]. By virtue of the aluminizing process used after the platinum is deposited on the surface of the superalloy by electroplating, two major types of structures can be categorized, inward and outward, as was described to the diffusion aluminide coatings. Deb and Boone [Ref. 9:pp. 12-16] have provided the following examination of the microstructures of platinum modified aluminide coatings on IN-738 (nickel base superalloy) substrate:

---

[2]For a comprehensive listing and review, see Ref. 18, p. 3; Ref. 11, pp. 10-11; Ref. 9, pp. 1-9.

1 Inward: The inward type Pt-Al coatings are formed using the LTHA aluminizing process after an electroplated platinum layer has been pre-diffused. Although the diffusion path of the aluminum through the platinum layer has not been conclusively determined, it does result in a high aluminum gradient across the Ni-Al coating. A minimum pre-aluminizing diffusion heat treatment produces a four zone microstructure: a high platinum content single phase $PtAl_2$ constitutes the surface zone, which has the outer intermediate zone underlying it that is either a platinum-rich precipitate in a Ni-Al matrix enriched in Al or an Al-rich NiAl precipitate in a continuous $PtAl_2$ phase. The inner intermediate zone is a single phase NiAl that is rich in Ni. The interdiffusion zone is the innermost zone, consisting of substrate phases and elements insoluble in β-(NiAl) formed when Ni is withdrawn from the Al-rich surface. Longer pre-diffusion heat treatments result in a three zone structure. The outer zone is $PtAl_2$ phase in a NiAl matrix rich in Al. The intermediate zone is a single NiAl phase and the innermost zone is the interdiffusion zone.

2 Outward: A HTLA aluminizing process produces the outward type Pt-Al coating. It has a lower Al gradient across the Ni-Al coating, theorized to result from aluminum diffusing inward until it forms a single NiAl phase containing low Pt and Al through which only Ni diffuses outward from the substrate to the pre-diffused Pt enriched layer. As in the inward type, the extent of the pre-aluminizing heat treatment affects the microstructure formed. The minimum heat treatment produces a two zone structure: the outer zone is a platinum rich $PtAl_2$ phase and the interdiffusion zone is beneath it. The typical structure following longer heat treatments has three zones. The surface zone has a Pt-rich precipitate in the Al-rich NiAl matrix. The intermediate zone is a single phase NiAl rich in nickel, void of any other phases or substrate elements, while the third zone is the interdiffusion zone.

D. RUMPLING

The observance of a surface macro-roughening of platinum modified aluminide coatings was first reported by Manley in conjunction with work he conducted on oxide scale adherence during cyclic oxidation testing [Ref. 22:p. 38]. This work was later published in an article by Deb et al [Ref. 23] This surface phenomena was termed rumpling. Strangman observed a similiar surface effect with certain overlay coating systems during cyclic oxidation burner rig testing, when subjected to intermediate temperature dwell periods [Ref. 24]. Manley's description of rumpling is of a kneaded surface texture with peak to peak distances on the order of 100 μm [Ref. 22:p. 38].

Manley concluded that rumpling was dependent on thermal cycling. Melt, isothermal and cyclic tests were performed. While rumpling did occur with substrate melting, it was on a much grosser scale and at significantly higher temperature (1200 C) than the rumpling he was investigating. The isothermal specimen did not exhibit rumpling, but the specimen cycled for the same time period did. [Ref. 22:pp. 39-40] This depencency on thermal cycling supports Strangman's hypothesis, suggesting that thermal expansion mismatch induced cyclic reversed creep plays an important role in the rumpling of diffusion aluminides and platinum modified coatings as well.

Coefficients of thermal expansion of oxides and some intermetallic coatings are generally lower than those of high temperature superalloys [Ref. 25:p. 4]. Vogel found the platinum aluminide coatings on IN-738 to be in a state of compression at room temperature from his data on ductile to brittle transition temperature (DBTT) and inherent ductilities of the coatings [Ref. 26]. This observation supports the above generality, the diffusion coating systems being tested having a lower coefficient of thermal expansion than the substrate IN-738 ($\alpha \sim 15.9 \times 10^{-6}/\circ C$) [Ref. 27:p. 142]. This mismatch most likely induces thermal stresses during temperature variation.

The magnitude of these stresses can be found, for an oxide layer of thickness t on a substrate of semi-infinite plate geometry, by

$$\sigma_{xx} = 0 \qquad \text{(eqn 2.2)}$$

$$\sigma_{yy} = \sigma_{zz} = -E_{ox}(\Delta\alpha\Delta T/(1-\upsilon_{ox})) \qquad \text{(eqn 2.3)}$$

where E_{ox} and υ_{ox} are Young's modulus and Poisson's ratio of the oxide, respectively, $\Delta\alpha$ is the coefficient of thermal expansion differential ($\alpha_{ox} - \alpha_m$) and ΔT is the temperature range ($T_{max} - T_{min}$). Douglas gives an induced compressive stress of $\sigma_{yy} \sim 1300$ MPa in an alumina scale ($E_{ox} \sim 300$ GPa, $\upsilon_{ox} \sim 0.26$, $\alpha_{ox} \sim 7.5 \times 10^{-6}/\circ C$) on a superalloy substrate ($\alpha_m \sim 14 \times 10^{-6}/\circ C$) with a temperature drop $\Delta T = 500$. [Ref. 27:p. 141] It is easily seen that the thermal stresses are proportional to the temperature differential and coefficient of thermal expansion mismatch. But they are reported to be independent of the heating or cooling rates, unless there is a very high cooling rate [Ref. 28].

The thermal stresses induced by cyclic operating conditions in a gas turbine add to the oxidation-induced growth stresses already present. The accompanying strains are what is believed to lead to rumpling. Strangman attributes the roughening he found in the overlay coatings to coating cyclic-reversed creep deformation produced by the thermal expansion mismatch strain between the coating layer and the substrate [Ref. 24]. It has been noted that at high temperatures ($T \geq 0.5\ T_m$), diffusional creep seems to be the mode of deformation most relevant for the strain rates involved during oxidation at high temprature [Ref. 27:p. 6].

It has been shown that coating thickness has an effect on crack propagation and therefore on thermal mechanical fatigue life: thicker coatings tend to favor crack propagation [Ref. 29]. Manley's data also indicated a coating thickness influence, but the reverse effect: thicker coatings rumpled less than thin coatings. This is postulated to be the result of the higher aluminum and platinum contents of the thicker coatings resulting in a 'stronger', more deformation resistant system. In fact, cyclic induced cracking was observed for the thicker, higher aluminum and platinum content coatings which could apparently not relieve the thermally induced strain by creep deformation. To study this surface roughening's relationship with the coating thickness parameter, testing of different coatings of two thicknesses was conducted.

III. EXPERIMENTAL PROCEDURES

A. APPARATUS

A horizontal (with respect to the ground) cyclic oxidation furnace rig was used to conduct the high temperature cyclic oxidation experiments. It has a three zone, 6.0 cm diameter tube, furnace with a 14.0 cm uniform hot zone at the temperature of interest. The specimens were moved automatically in and out of the hot zone by a chain drive. The cycle is variable and controlled by a timer with the number of cycles documented by a counter. The cycle frequency was set for a one hour exposure at temperature followed by a ten minute air cool, with the furnace hot zone being maintained in these tests at a temperature setting of 1100 C $\pm$5 C. Figure B.2 shows the furnace rig.

B. SPECIMEN PREPARATION

Specimens were prepared using a commercial nickel base superalloy, IN 738, as the substrate; Table II presents its nominal composition. The specimens were in the form of cast and ground pins, lengths on the order of 8.0-9.0 cm, with two ranges of diameters: 0.50-0.58 cm and 0.70-0.80 cm. The substrate pins were commercially platinum electroplated to a thickness of 7.0-8.0 μm. After their return, the pins were individually encapsulated in quartz tubing and vacuum sealed. Using one of the adopted standard pre-aluminizing heat treatments outlined in Table III, each pin was diffused. The pins were then sent out for aluminizing by one of two processes used for this study. The first process is the low activity high temprature method which inwardly diffuses aluminum onto a substrate, resulting in an inward type aluminde coating system. The high activity low temperature process chosen as the second process results in an outward type aluminide coating system by incorporating aluminum through outward diffusion of nickel from the substrate. Unplated pins were also aluminized by these processes to serve as appropriate baselines. All pins were given a post-aluminizing diffusion treatment of four hours at 1080 C. Upon return, the specimens were cut into approximately 2.5 cm test lengths. To prevent excessive localized oxidation attack, a commercial, brush-on, aluminum slurry repair coating was applied to uncoated surfaces. The specimens were categorized according to the codes in Table IV.

Two specimens with a platinum aluminide coating prepared by an intermediate temperature, intermediate activity process were also tested. One of the specimens received post-aluminizing smoothing, using a series of diamond abrasive pastes on felt tips. This specimen was designated smooth; the as-received specimen was designated rough.

A listing of the specimen numbers and their codes is presented in Table V.

C. EXPERIMENTAL TESTING

The specimens were placed in the specimen boat of the horizontal cyclic oxidation furnace rig, using a holder made of a high temperature castable ceramic. They were cycled under normal atmospheric conditions for two hundred seventy five cycles (275 hours). After the first twenty five cycles and for fifty cycle intervals after that, the specimens were removed and examined for signs of oxide spallation and color changes (an indication of the formation of alternate oxides). At various intervals, low magnification surface photomicrographs and cross-sectional cuts were used to record coating microstructural and surface morphological changes.

D. DATA ANALYSIS

Lineal roughness measurements, taken from coating cross-section photomicrographs at 250X, were used to characterize changes in the coating system profiles. Lineal roughness is defined as the ratio of the actual surface profile trace length to the normal surface projection length [Ref. 30]. A graphical definition of lineal surface roughness is shown in Figure B.1. The accuracy for the lineal roughness measurements was estimated to be within ± 0.02. Lineal roughness measurements were averaged when more than one micrograph was taken. The lineal surface roughnesses for each specimen are listed in Table VI.

IV. RESULTS AND DISCUSSION

A. GENERAL OBSERVATIONS

The horizontal cyclic oxidation rig performed well during testing, the temperature in the hot zone remained at 1100 C ±5 C for the duration of the test. The set-up of the rig provided steep heating and cooling gradients, shown in Figure B.1.

Several specimen types initially planned for testing were unavailable as a result of spallation due to static fatigue. This problem is not infrequent and is another indication of the highly stressed state of the surface layer and the low ductility of some structural/compositional types. Another problem is the difficulty in obtaining controlled, reproducable structures for testing. Variables in production processes, even slight, are found to have a strong effect on a coating's final microstructure and potentially its performance. To offset this variable, detailed microprobe analysis should be conducted on all initial structures.

Considerable oxide spallation occured on the two baseline specimens, the unmodified aluminide coatings. The spallation was over the entire specimen. The platinum modified aluminide coatings only showed localized spalling toward the end of the testing, if at all.

B. RUMPLING

The surface plastic instability phenomena known as rumpling was observed with varying degrees of magnitude in all specimens that underwent the cyclic oxidation testing. Rumpling occurred irrespective of the aluminizing process used or the thickness of the coating. Figure B.3 shows a low magnification view of a diffusion aluminide coating and three standard platinum aluminide coatings, all of which underwent the LTHA aluminizing process; these were thin coatings ($\sim$30-50μm). The surface plastic deformation is seen as the rumpled effect. The surfaces of four standard platinum aluminides (HTLA aluminizing process) are shown in Figure B.4 at low magnification; these were all thick coatings ($\sim$50-70μm). Again, rumpling is evident. The appearance of rumpling on the unmodified aluminides, as shown here and in subsequent figures, is a significant point as it had been postulated that possibly the excellent adherence of the low coefficient of thermal expansion α-Al_2O_3 scale was in some way responsible for the increased rumpling observed for the platinum modified

aluminides and the active element containing overlays. The observations of rumpling on the unmodified coatings suggest that oxide adherence effects on rumpling may be minor.

The dependence of rumpling on thermal cycling can clearly be seen by examination of Figure B.5 and Figure B.6. The first figure demonstrates the increase in rumpling with thermal cycling for a thin standard platinum aluminide coating. The latter figure of a thick standard platinum aluminide coating, while not showing the same degree of rumpling as for the thin platinum aluminide coating, still clearly demonstrates rumpling as an increasing function of thermal cycling. Both baselines (unmodified aluminide coatings), for the inward and outward aluminizing processes, show measurable amounts of rumpling with thermal cycling, see Figures B.7 and B.8.

Quantitative roughness measurements made from photomicrographs were plotted as a function of thermal cycles. These plots present several interesting results. Figure B.9 shows an increase in rumpling with increased diffusion treatment time for the inward type platinum aluminide coatings of the same thickness. Outward type thin coatings also show an increase in rumpling with diffusion times, see Figure B.10. Figure B.11 and B.12 are photomicrograhps of thin inward and outward type coatings, respectively, which give the cross-sectional aspect of the surface instability. For thick coatings, Figure B.13 shows the same dependence of rumpling magnitude on diffusion times for outward coatings, with the exception of the first diffusion treatment, which is half an hour at 870 C. Cross-sectional views of the rumpling of these specimens are shown in Figure B.14; Figure B.15 displays an increase in rumpling for longer diffusion treatment times for thick inward coatings. While decreased aluminum in the coating decreases the thermal expansion coefficient mismatch, all the data indicate that this must be more than offset by a concomittant decrease in strength.

A possible explanation for the greater tendency for rumpling with longer diffusion treatment times is the amount of aluminum and platinum present in each coating. Microprobe analysis data of similiarly prepared inward type coatings [Ref. 31:pp. 26-47] shows a decrease in total aluminum content throughout the coating as diffusion treatment times are increased; the unmodified aluminide baseline specimen indicated the relative least amount of aluminum. If it is the higher aluminum content that is adding strength to the coating and lowering its plasticity, then it would be expected that the specimens which had longer diffusion times would rumple more. Microprobe analysis data [Ref. 31:pp. 26-47] of similiarly prepared outward type

coatings were not as conclusive as far as the aluminum level is concerned; there is not as rapid an initial decrease but the data clearly shows reduced aluminum and movement of platinum from the surface to the substrate. A more detailed study of compositional changes which occur during exposure is needed.

The roughness measurements also showed thinner coatings rumpling more than thicker coatings of the same composition, as previously found by Manley. Figure B.16 shows for two different diffusion treatments how the thinner version rumpled more than the thicker one. Figure B.17 shows even more dramatically the difference 2n the magnitude of the rumpling of the coatings of two thicknesses. The dependency of rumpling on the thickness of the coating led to an additional effect: thinner coatings rumpled sooner. Thick coatings demonstrated no or little rumpling halfway through the duration of the cyclic testing, whereas the thinner versions started rumpling immediately, see Figure B.18. This influence of thickness of the coating is once again believed to be a function of the aluminum and platinum contents of the coating; by their very nature, thicker coatings have an increased aluminum content and take longer to diffuse down through the coating. This suggests the possibility of a critical strength (aluminum/platinum content) for deformation. The thicker coatings appear to resist rumpling until their surface content of aluminum and platinum have been reduced to some level where plastic deformation can be effected. While no cracks were seen in this series of specimens, if the level of strains are sufficient in the early stage of testing and the coating lacks sufficient ductility, cracking can occur as reported by Manley. Although the thicker coatings did not rumple as soon, their growth rates after rumpling was initiated paralleled those of the thin coatings.

The data is inclusive to support a hypotheis concerning the performance of inward vs outward type coatings in regards to rumpling. This may be because during the testing at 1100 C we are simultaneously heat treating and diffusing the coating; then any initial structural differences between the inward and outward coatings rapidly disappear.

These variations in rumpling magnitude and occurence are consistent with Manley's data [Ref. 22:pp. 43-44] with a difference in data stemming from rumpling rate observations. This data show a linear increase in rumpling while Manley found a plateau in the amount of rumpling achieved by any one specimen, roughly corresponding to the onset of spallation, most noticable with the unmodified aluminide coatings. In this study while spallation of the baseline specimens did occur, no

plateaus were noted. Localized spalling ocurred later in the test on some of the platinum aluminide specimens, but again no plateaus were reached.

The effect of initial surface topology on rumping was a consideration because of the apparent similarities of the plated surface nodules and the rumpling spatial frequency. Therefore samples were post-coating smoothed. Data obtained from the rough and smooth specimens showed no significant difference in the amount of rumpling occurring on each specimen's surface. Figure B.19 in fact shows a slight increase in rumpling for the smooth specimen, while Figure B.20 presents cross-sectional views of the two specimens. This leads to the suggestion that post-aluminizing smoothing does not decrease the amount of rumpling, which further suggests that initial surface roughness plays no role in rumpling. This is further validated by Farrell's work on the oxide adherence characteristics of rough and pre-aluminizing smoothed specimens of platinum alumnide coatings on IN-738; again, she found no significant difference in the amount of rumpling between rough and smooth specimens [Ref. 32].

C. MICROSTRUCTURAL CHANGES

Examination of high magnifacation photomicrographs of cross-sectional views of the coating structures shows a rapid transformation of the two phase structures into single phase structures upon thermal cycling. Type 2IIA and Type 3IIA are two phase coatings in the as-formed condition, Figure B.21 presents an example of this transition to a single phase. Comparison of the structural transition in both inward and outward coatings with the longest diffusion treatment times can be made with Figures B.22 and B.23, it is readily seen that these coatings are initially two phase but make the transition to a single phase upon thermal exposure. This indicates that cyclic testing is actually being conducted on single phase structures with varying distributions of aluminum and platinum for all the initial coating variations. This indicates a compositional effect rather than a structural effect. But regardless of this transformation, a formerly two phase structure's rumpling rate does not change to match that of a structure that was initially single phase.

β(NiAl) phase degradation can be clearly seen in the diffusion aluminide coatings, in both the inward and outward baseline specimens. By halfway through the testing period (~150 hours), gamma and gamma prime phases are present, see Figures B.24 and B.25, indicating a significant reduction in the aluminum level, i.e. the β(NiAl)

phase with its reservoir of aluminum. The presence of γ and γ' are not in themselves detrimental when a sufficient amount of β remains. However, γ' with its greater solubility for potentially detrimental substrate elements can serve to transport these elements form the substrate if γ' channels (spikes) are formed throughout the β phase. Preliminary formation of these spikes can be seen in Figure B.24b. The platinum aluminides did not demonstrate such a marked degradation of the β(NiAl) phase, as evidenced in Figure B.26. One obvious function of the platinum is to reduce the loss of aluminum via spallation, while another function could be to stabilize the presence of the β(NiAl) phase even with lower aluminum levels and/or reduce the propensity to form γ' spikes in/through the β phase.

The effect of the surface zone of lower aluminum γ and γ' phases on rumpling is not known, although if strength is the controlling factor, a greater amount of plastic deformation would be expected with the appearance of the γ and γ' and this is in fact observed. It is interesting to note that while Manley showed more rumpling for the platinum aluminides, which suggests a coefficient of thermal expansion effect, the present test results with modified and unmodified coatings of similar thicknesses (and aluminum levels) showed a greater amount of rumpling for the unmodified coatings, which are found to loose aluminum at the surface at a greater rate.

V. CONCLUSIONS

The experimental results and subsequent discussion support the following conclusions:

1 The surface deformation phenomena known as rumpling is a function of thermal cycling. The increasing rumpling rate was seen to be linear, with no plateaus reached by the test's termination at two hundred seventy five cycles. At constant thickness, a higher aluminum content decreased the amount of rumpling.

2 It was further found that rumpling is a function of coating thickness: thin coatings rumple more and at a lower number of thermal cycles than thicker coatings of the same coating type.

3 Post-aluminizing smoothing has no significant effect on rumpling.

4 Coatings with an initial two phase microstructure rapidly transformed into single phase structures upon thermal cycling. Therefore, regardless of pre-aluminizing diffusion treatments, the structures actually tested were all single phase, with different platinum and aluminum distributions and corresponding rumpling rates.

APPENDIX A

TABLES

TABLE I

OXIDE-METAL VOLUME RATIOS

Protective oxides	Nonprotective oxides
Be--1.59	Li--0.57
Cu--1.68	Na--0.57
Al--1.28	K--0.45
Si--2.27	Ag--1.59
Cr--1.99	Cd--1.21
Mn--1.79	Ti--1.95
Fe--1.77	Mo--3.40
Co--1.99	Cb--2.61
Ni--1.52	Sb--2.35
Pd--1.60	W--3.40
Pb--1.40	Ta--2.33
Ce--1.16	U--3.05
	V--3.18

TABLE II

IN-738 COMPOSITION (WEIGHT PERCENT)

Ni	Cr	Co	Mo	W	Ti	Al
bal.	16.0	8.5	1.75	2.6	3.4	3.4

Nb	Ta	C	B	Zr	Fe
0.9	1.75	0.17	0.01	0.10	0.5 max

Mn	Si
0.2 max	0.3 max

TABLE III

NPS STANDARD PRE-ALUMINIZING HEAT TREATMENTS*

Code	Treatment
1	1/2 hour @ 870 C (1600°F)
2	2 hours @ 980 C (1800°F)
3	3 hours @ 1040 C (1900°F)
4	4 hours @ 1080 C (1975°F)

* All heat treatments were followed by static air cooling to room temperature

TABLE IV

CODING SYSTEM FOR PLATINUM ALUMINDE AND ALUMINIDE COATINGS

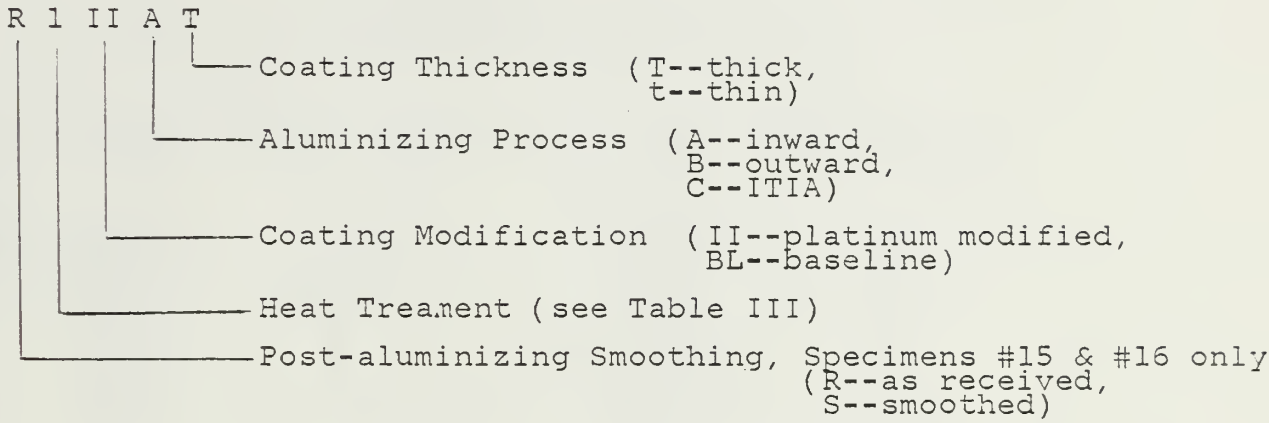

TABLE V

SPECIMEN LISTING

Specimen No.	Code	Specimen No.	Code
1	BLA	8	1IIBT
2	1IIAt	10	2IIBT
3	2IIAt	11	3IIBt
4	3IIAt	12	3IIBT
17	3IIAT	13	4IIBT
5	4IIAT	14	4IIBT
6	BLB	15	RIIC
7	1IIBt	16	SIIC

TABLE VI

CYCLIC EXPOSURE LINEAL ROUGHNESS DATA

Coating Specimen No.	Code	(cycles):	Lineal Roughness 0	150	275
1	BLA		1	1.0682	1.0909
2	1IIAt		1	1.0227	1.0909
3	2IIAt		1	1.0909	1.2727
4	3IIAt		1.0091	1.1136	1.1818
17	3IIAT		1	1.0454	-
5	4IIAT		1	1.0909	1.1818
6	BLB		1	1.0773	1.1364
7	1IIBt		1	1.0454	1.0909
8	1IIBT		1	1.0454	1.0909
10	2IIBT		1	1	1.0227
11	3IIBt		1	1.0682	1.0909
12	3IIBT		1	1	1.0864
13	4IIBT		1	1.0454	1.0909
14	4IIBT		1	1.0454	1.0909
15	RIIC		1	1.0091	1.0909
16	SIIC		1	1.0182	1.1091

APPENDIX B
FIGURES

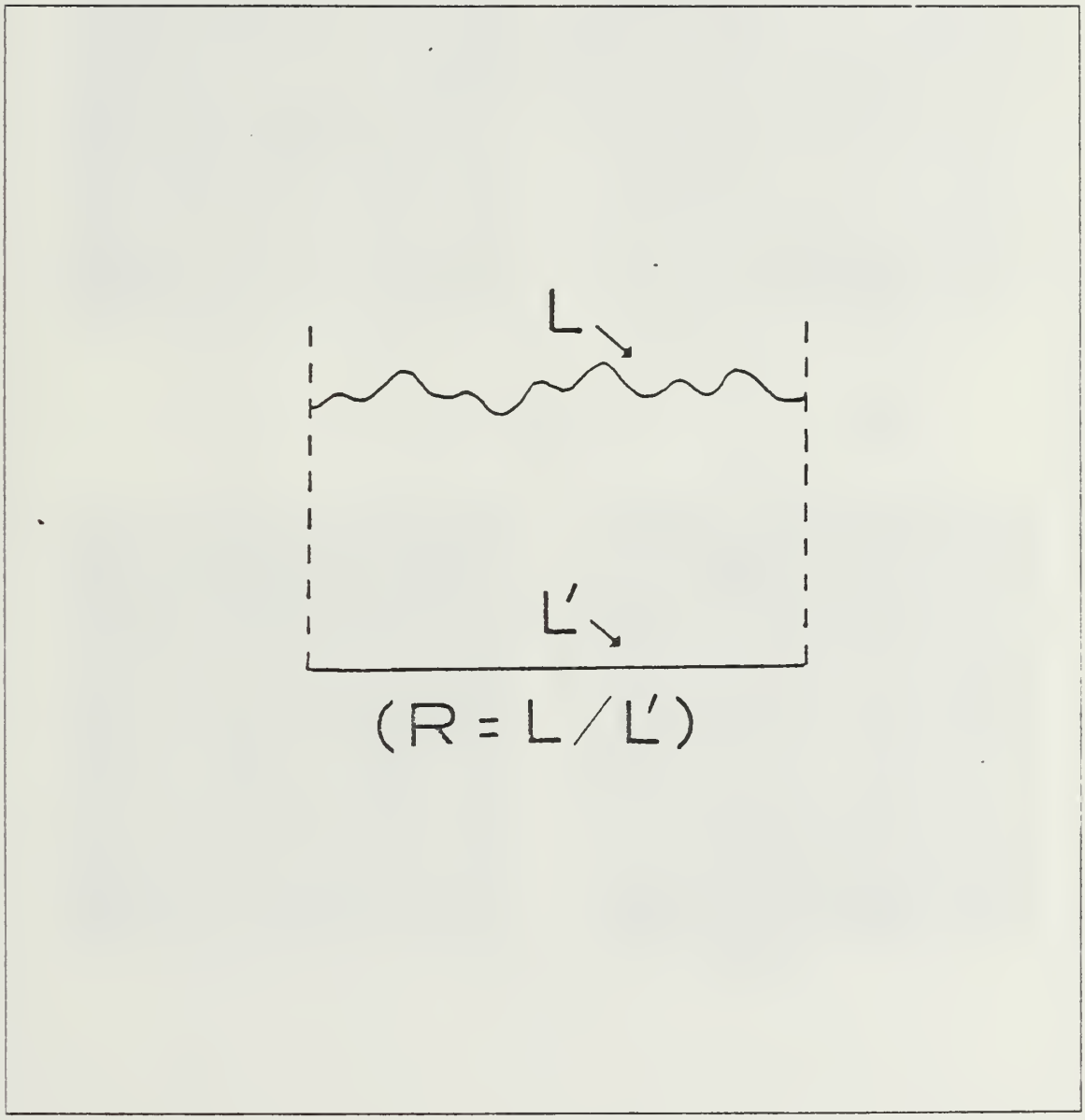

Figure B.1 Lineal Surface Roughness Measurement.

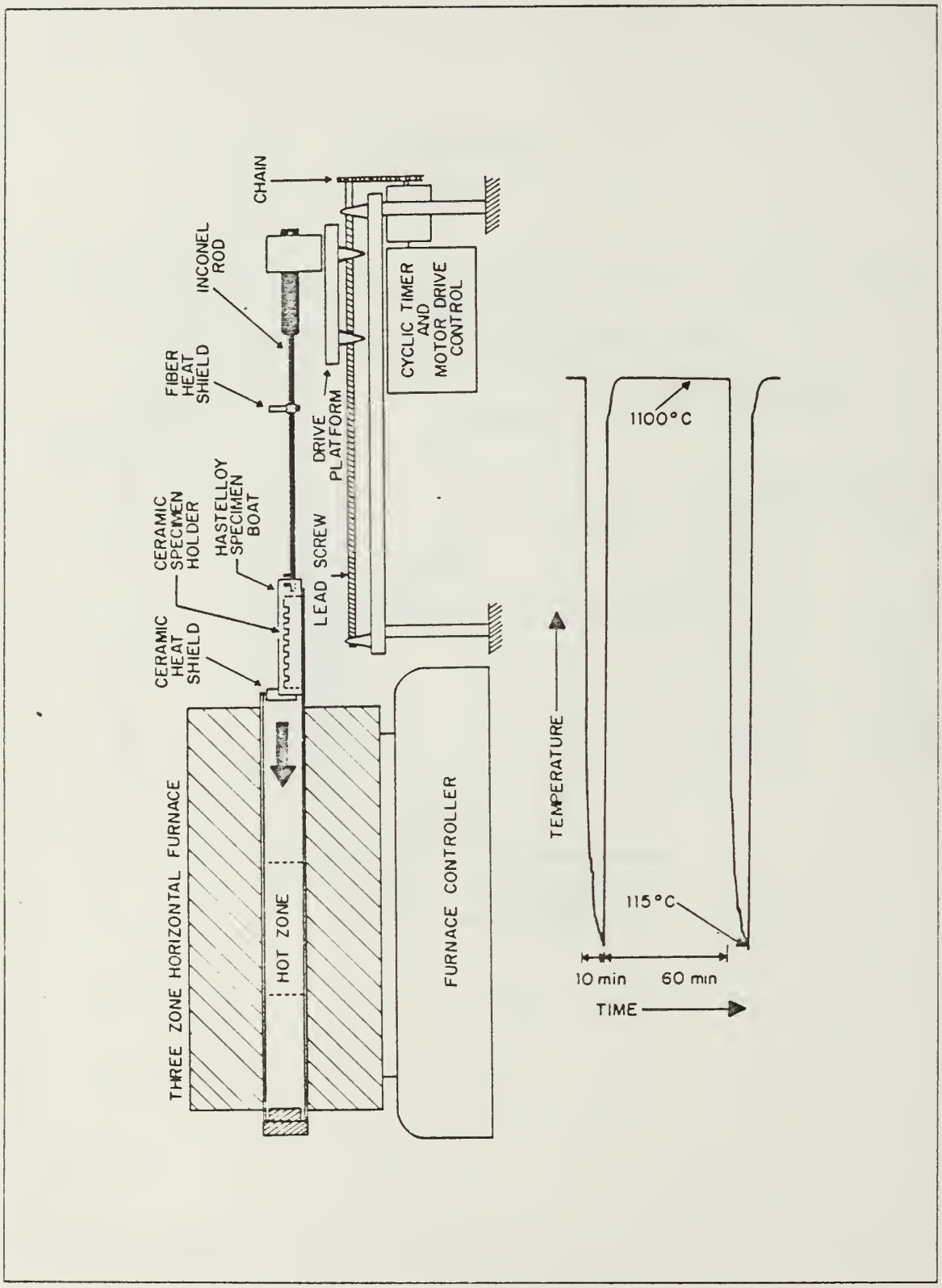

Figure B.2 Horizontal Cyclic Oxidation Rig and Associated Thermal Cycle.

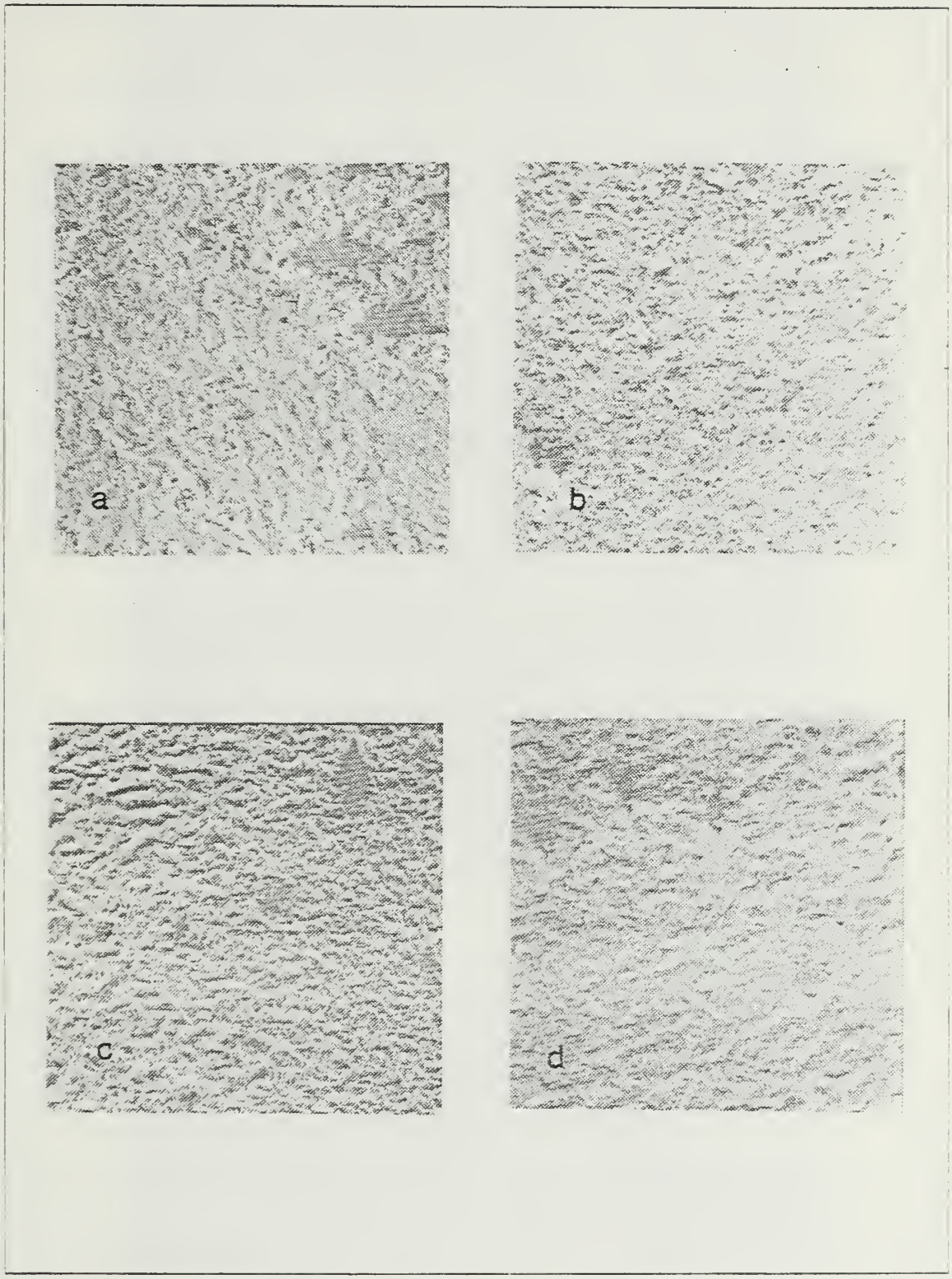

Figure B.3 Rumpled Baseline and Platinum Aluminide Specimen Surfaces, 275 Cycles (32 ×): a) BLA, b) 1HAt, c) 2HAt, d) 3HAt.

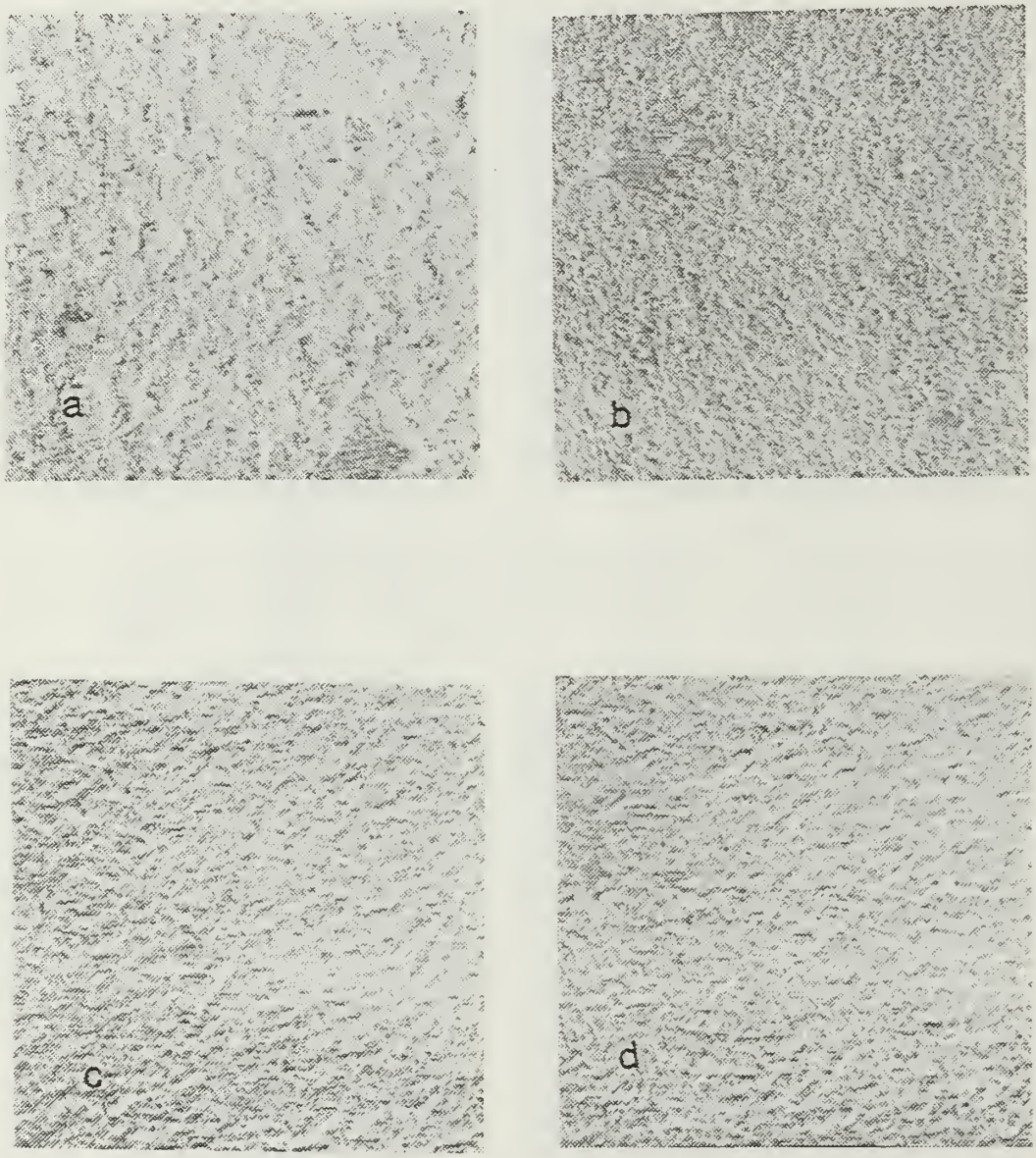

Figure B.4 Rumpled Platinum Aluminide Specimen Surfaces, 275 Cycles, (32×): a) 1HBT, b) 2HBT, c) 3HBT, d) 4HBT.

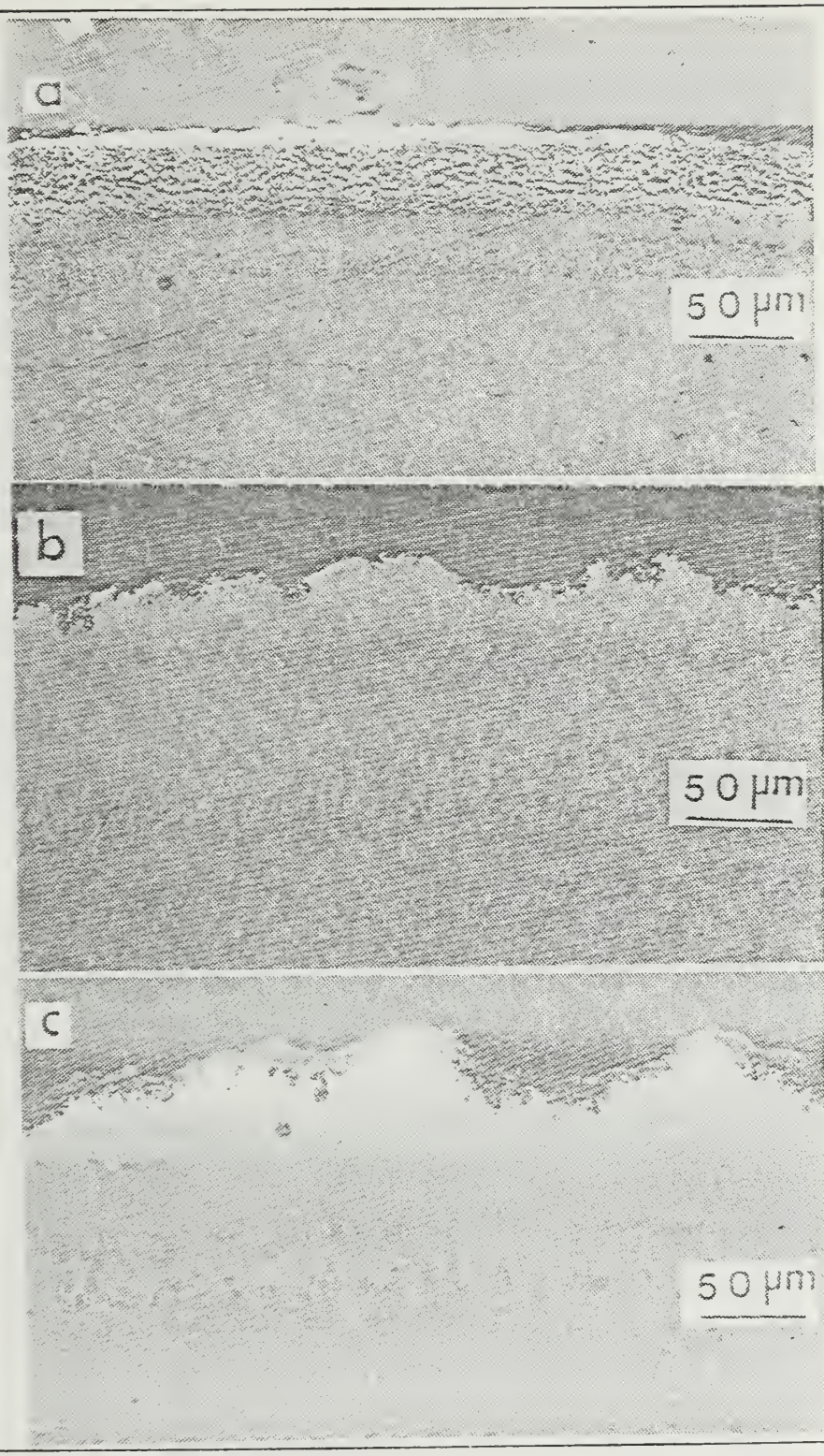

Figure B.5 Rumpling During Thermal Cycling for the Platinum Aluminide Coating 311Bt, (250 ×): a) 0 cycles, b) 150 cycles, c) 275 cycles.

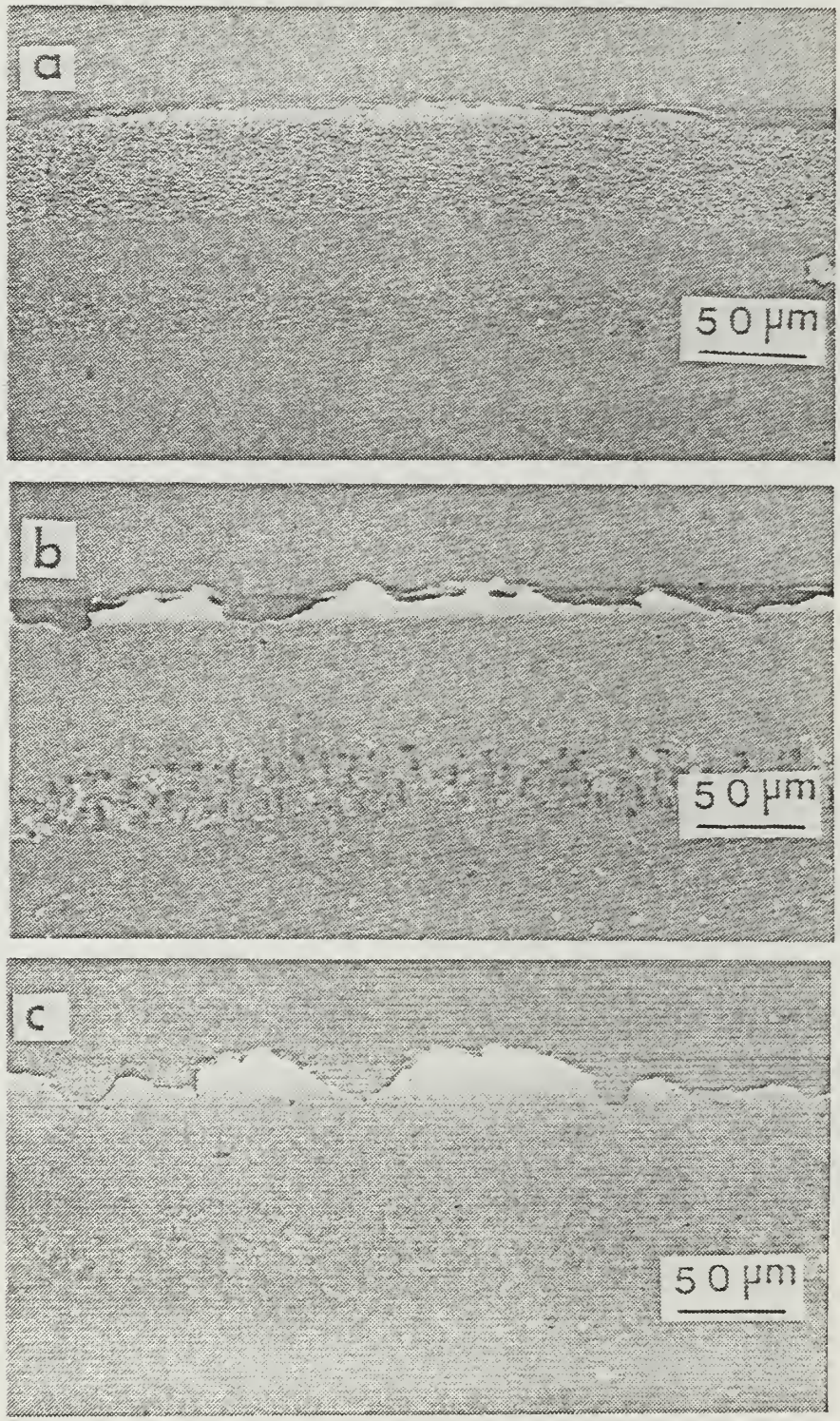

Figure B.6. Rumpling During Thermal Cycling for the Platinum Aluminide Coating 41BT, (250 ×): a) 0 cycles; b) 150 cycles; c) 275 cycles.

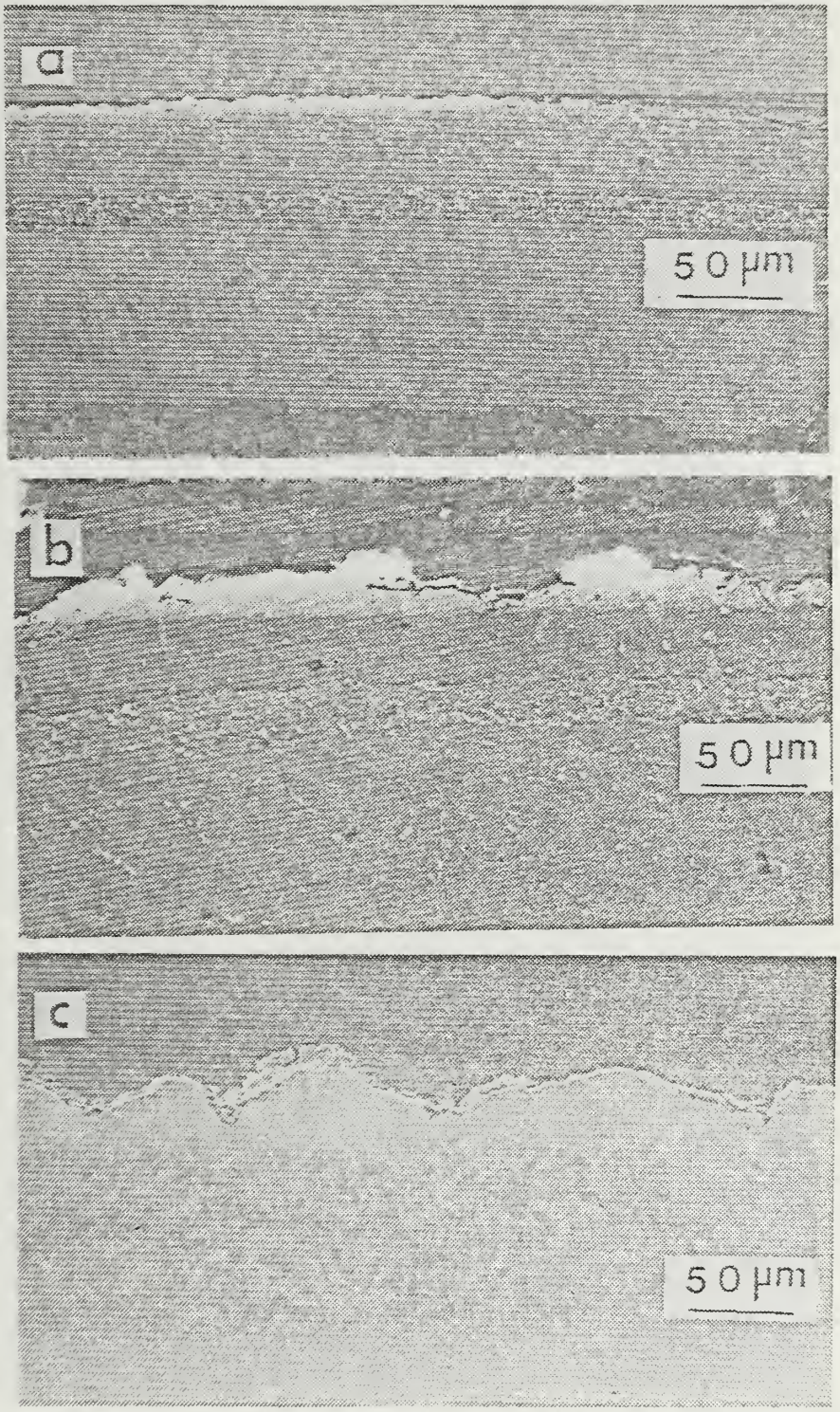

Figure B.7 Rumpling During Thermal Cycling for the Inward Baseline Coating BLA, (250 ×): a) 0 cycles, b) 150 cycles, c) 275 cycles.

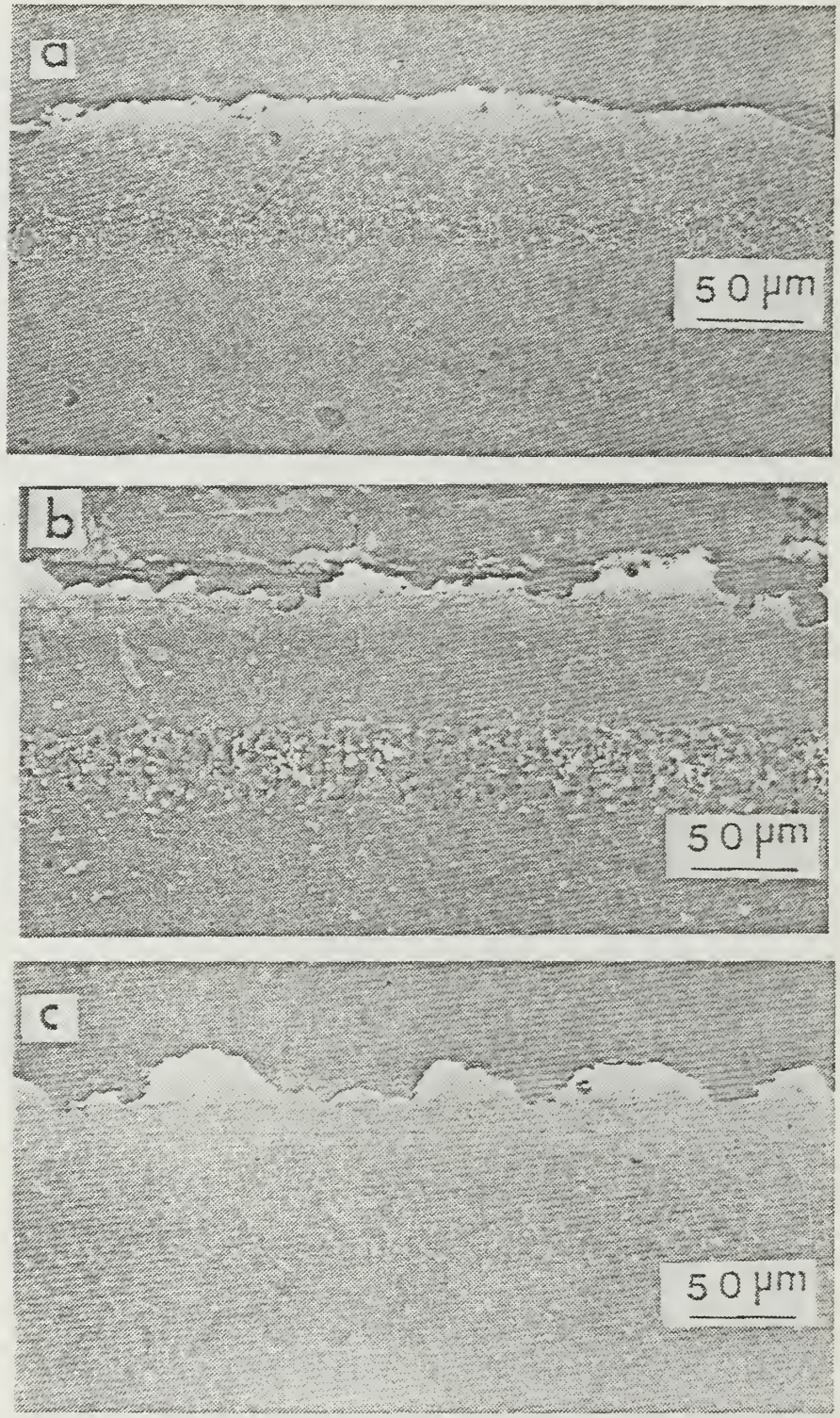

Figure B.8 Rumpling During Thermal Cycling for the Outward Baseline Coating B1.B, (250 ×): a) 0 cylces, b) 150 Cycles, c) 275 cycles.

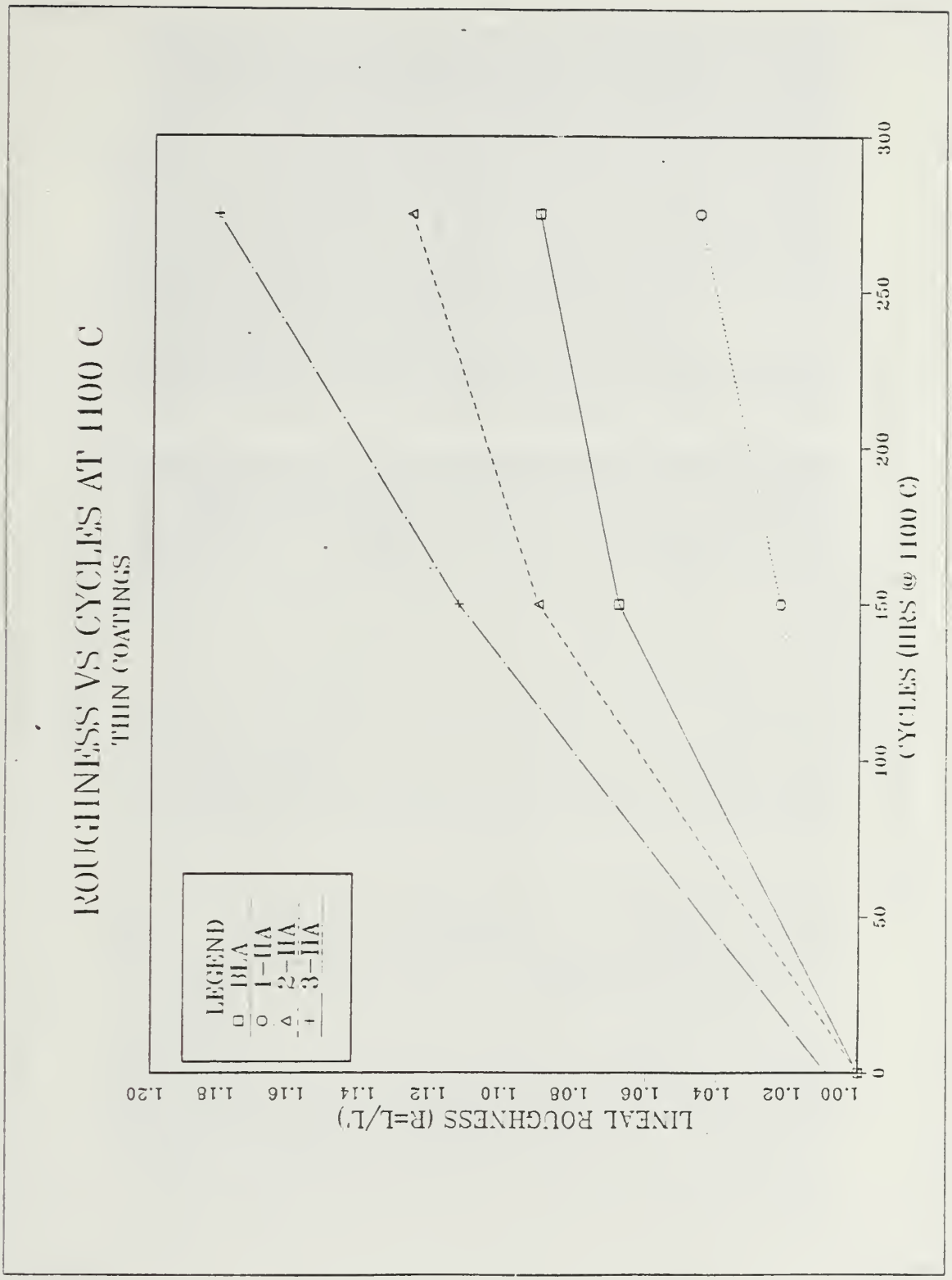

Figure B.9 Plot of Lineal Roughness versus Cyclic Exposure for Thin Inward Platinum Aluminide Coating and Baseline Specimens.

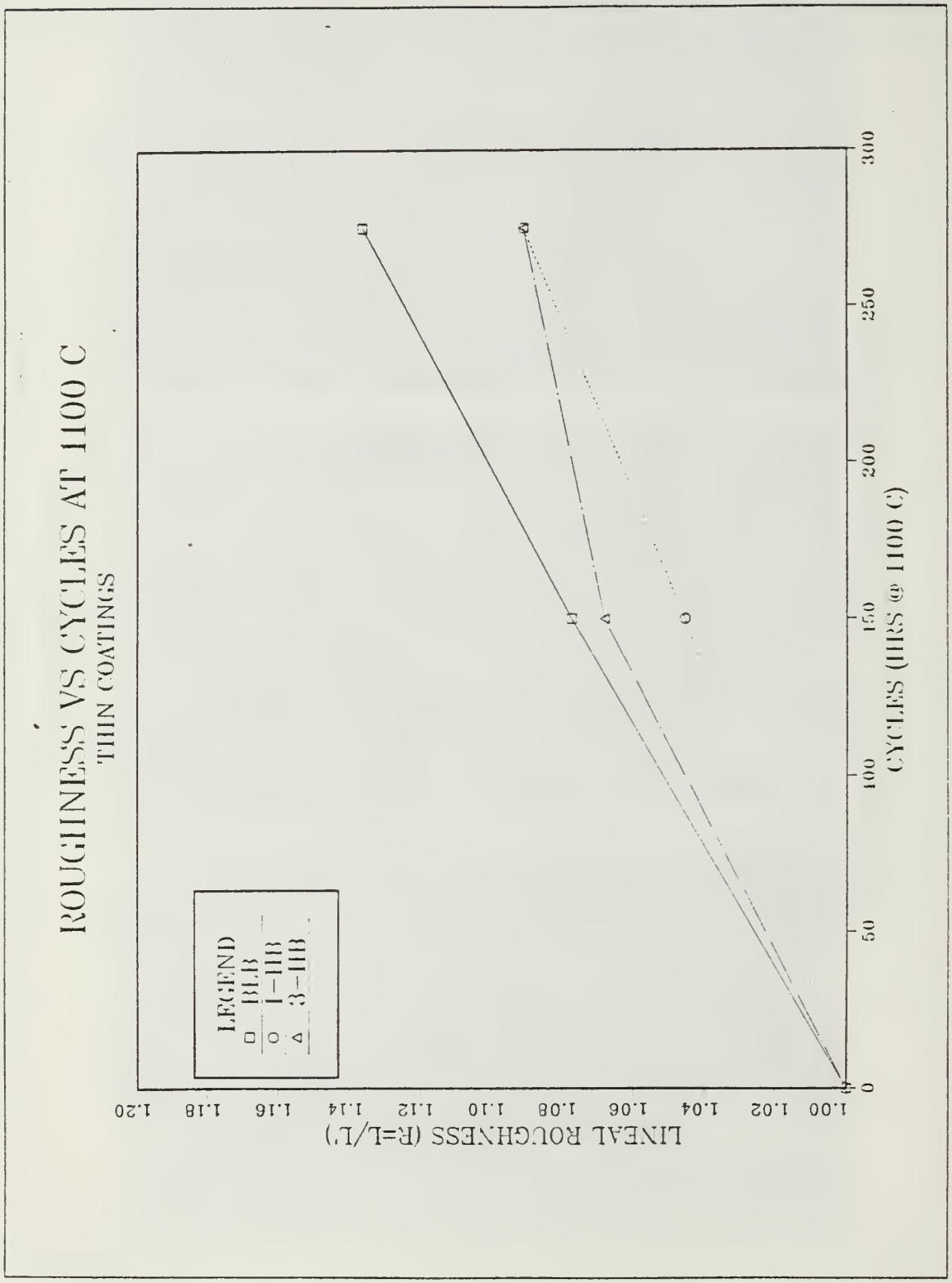

Figure B.10 Plot of Lineal Roughness versus Cyclic Exposure for Thin Outward Platimum Aluminide Coating and Baseline Specimens.

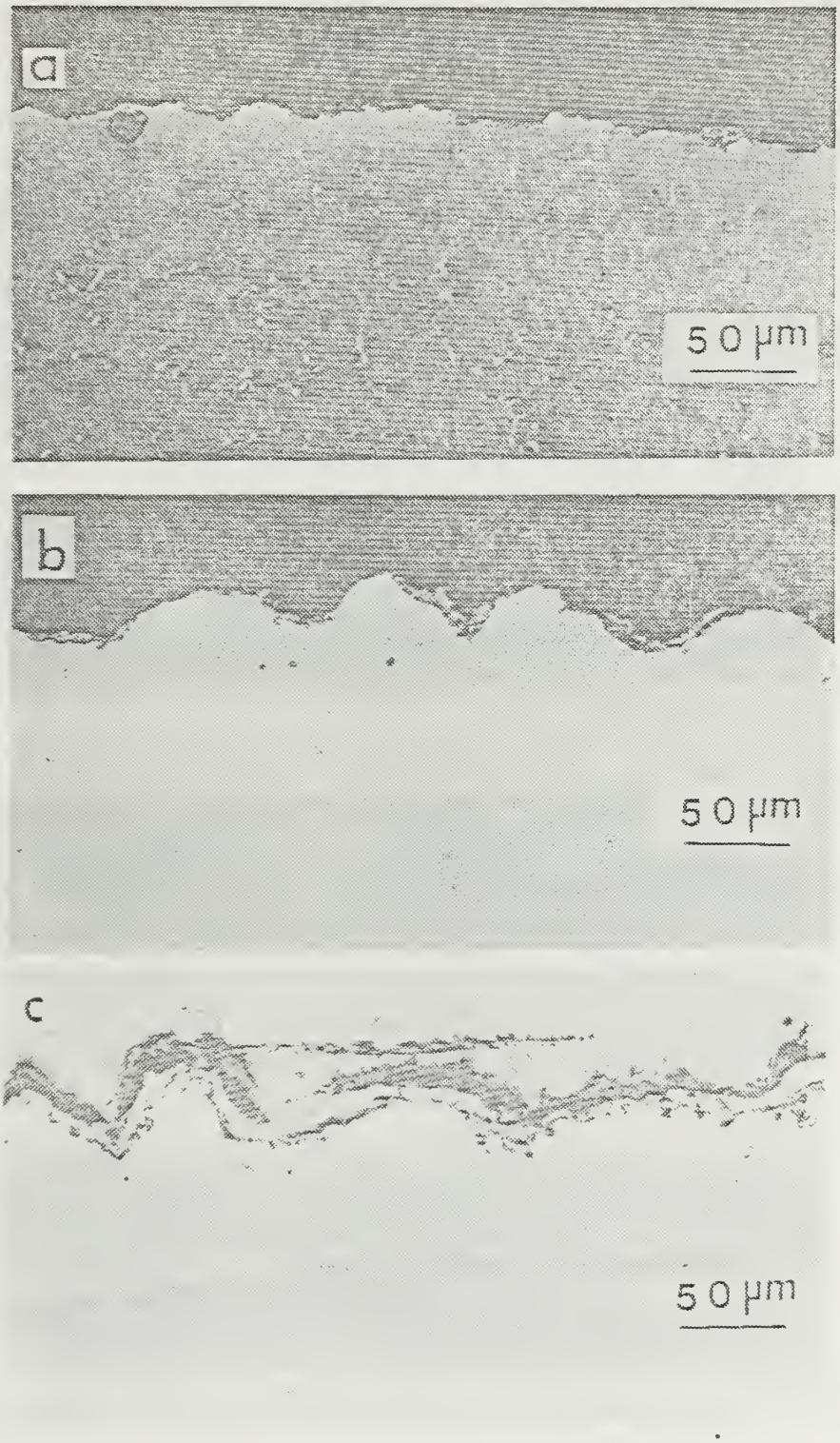

Figure B.11 Rumpling Comparison of Thin Inward Platinum Aluminide Coatings 275 Cycled, (250 ×): a) 1HAt, b) 2HAt, c) 3HAt.

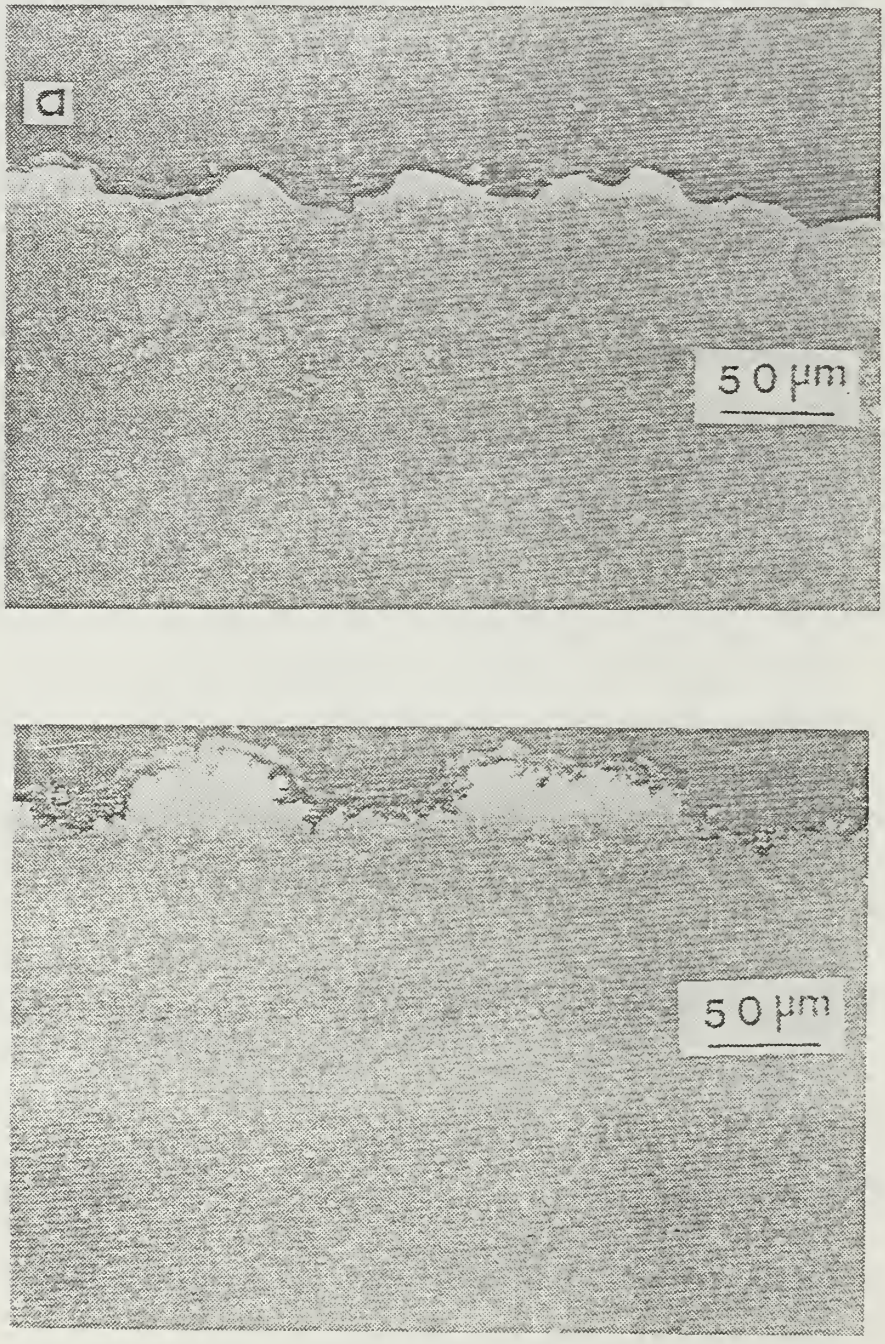

Figure B.12 Rumpling Comparison of Thin Outward Platinum Aluminide Coatings 275 Cycles, (250×): a) 1HBt, b) 3HBt.

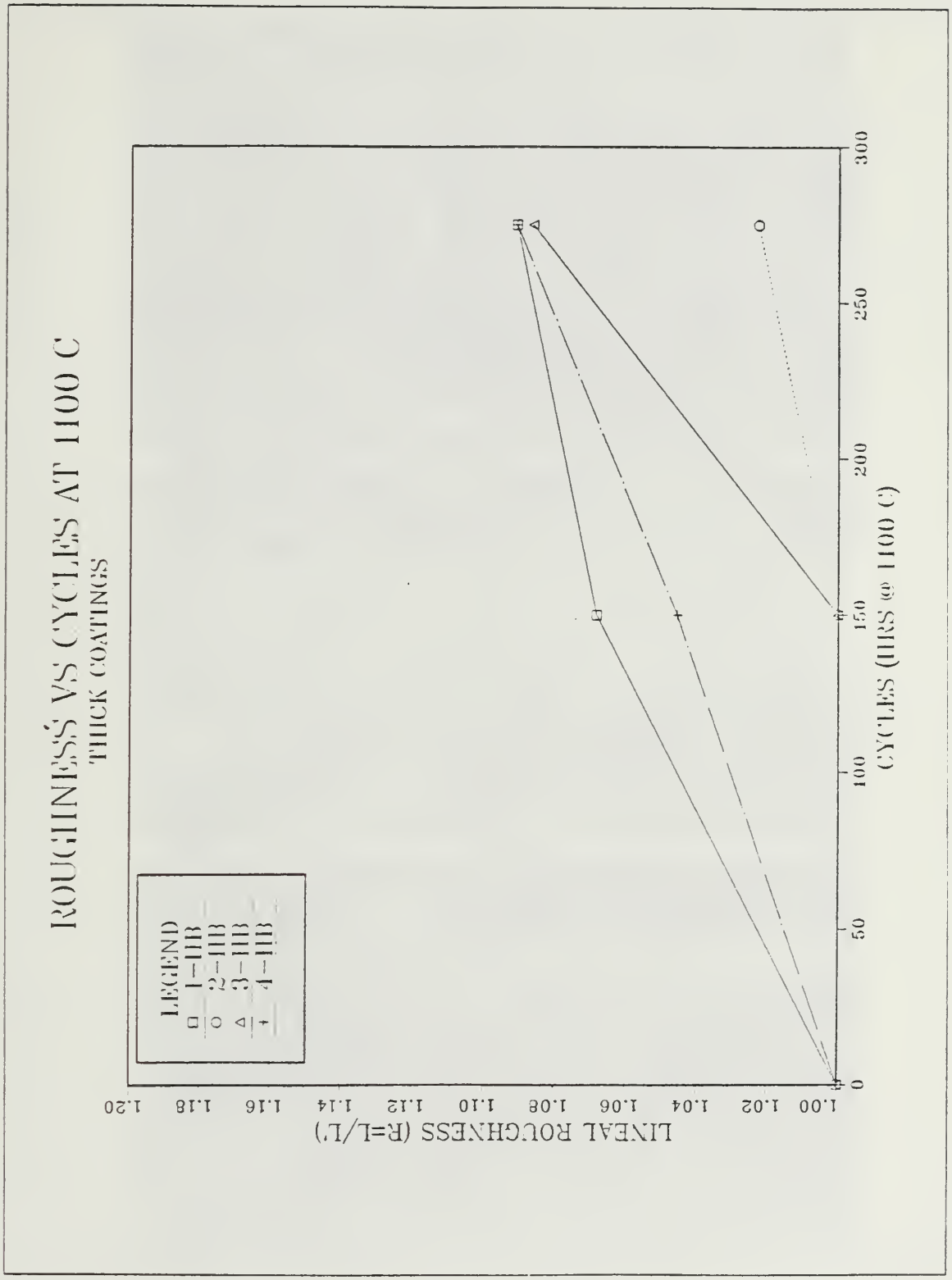

Figure B.13 Plot of Lineal Roughness versus Cyclic Exposure for Thick Outward Platinum Aluminide Coating Specimens.

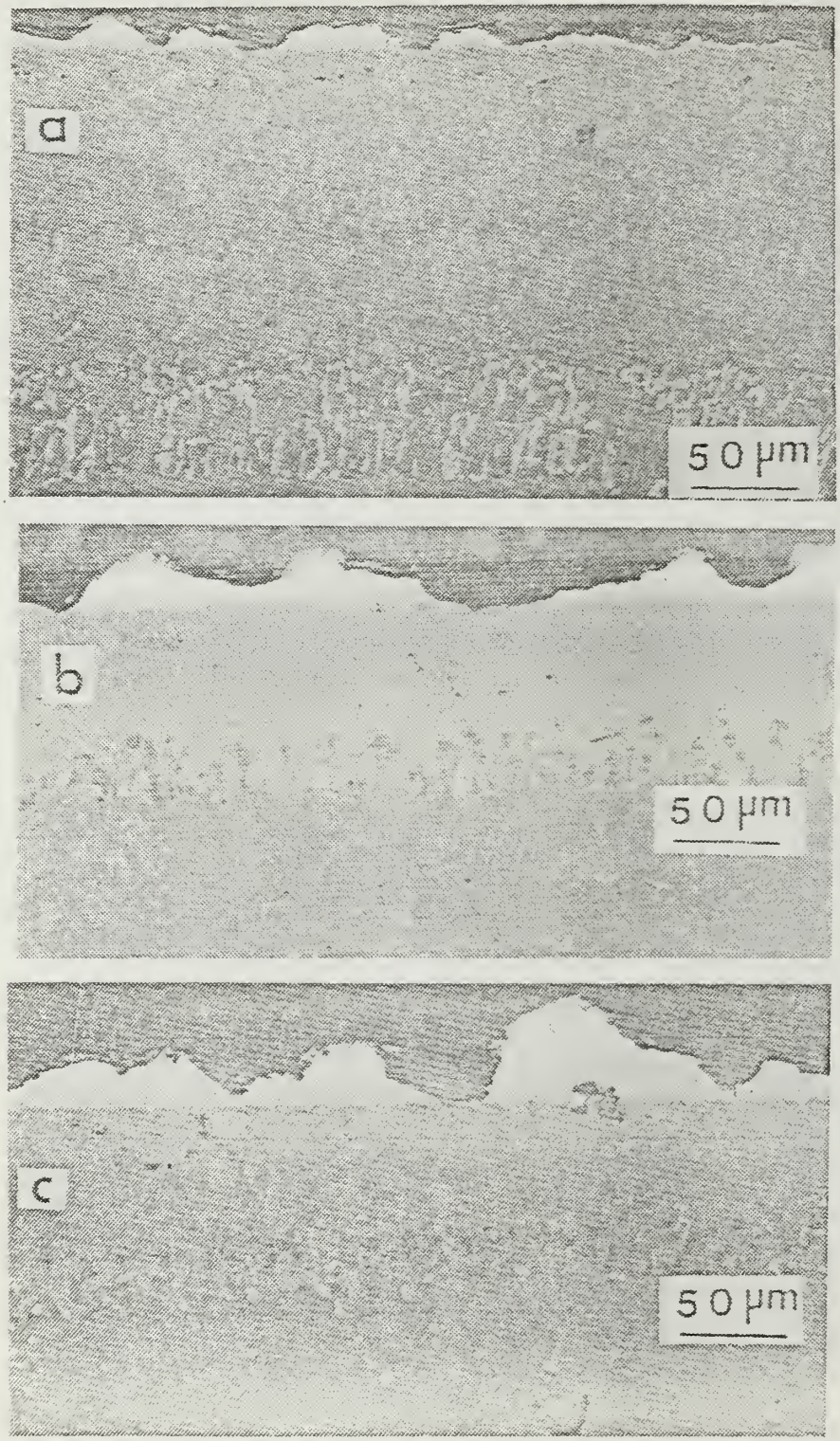

Figure B.14 Rumpling Comparisons of Thick Outward Platinum Aluminide Coatings 275 Cycles, (250 ×): a) 2HBT, b) 3HBT, c) 4HBT.

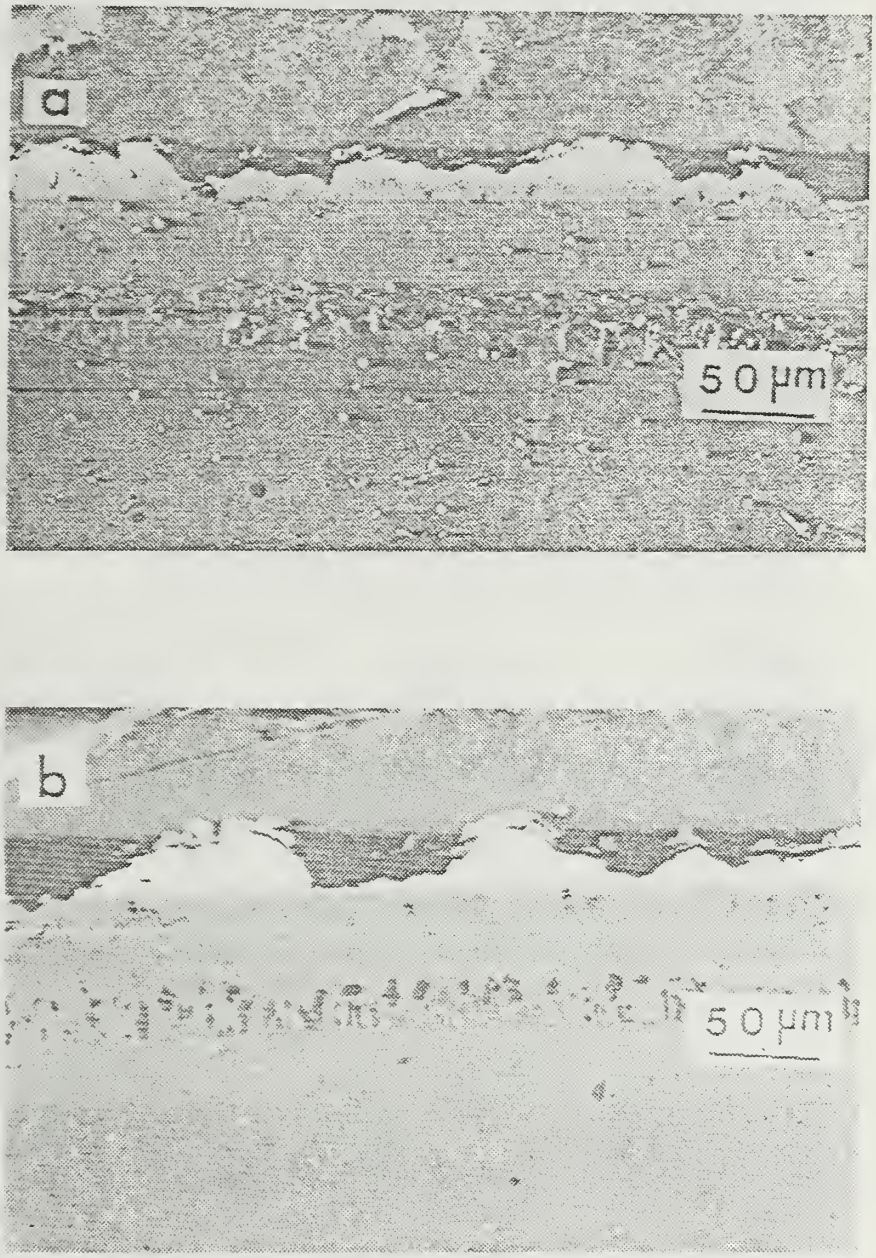

Figure B.15 Rumpling Comparisons of Thick Inward Platinum Aluminide Coatings 275 Cycles, (250 ×): a) 3HAT, b) 4HAT.

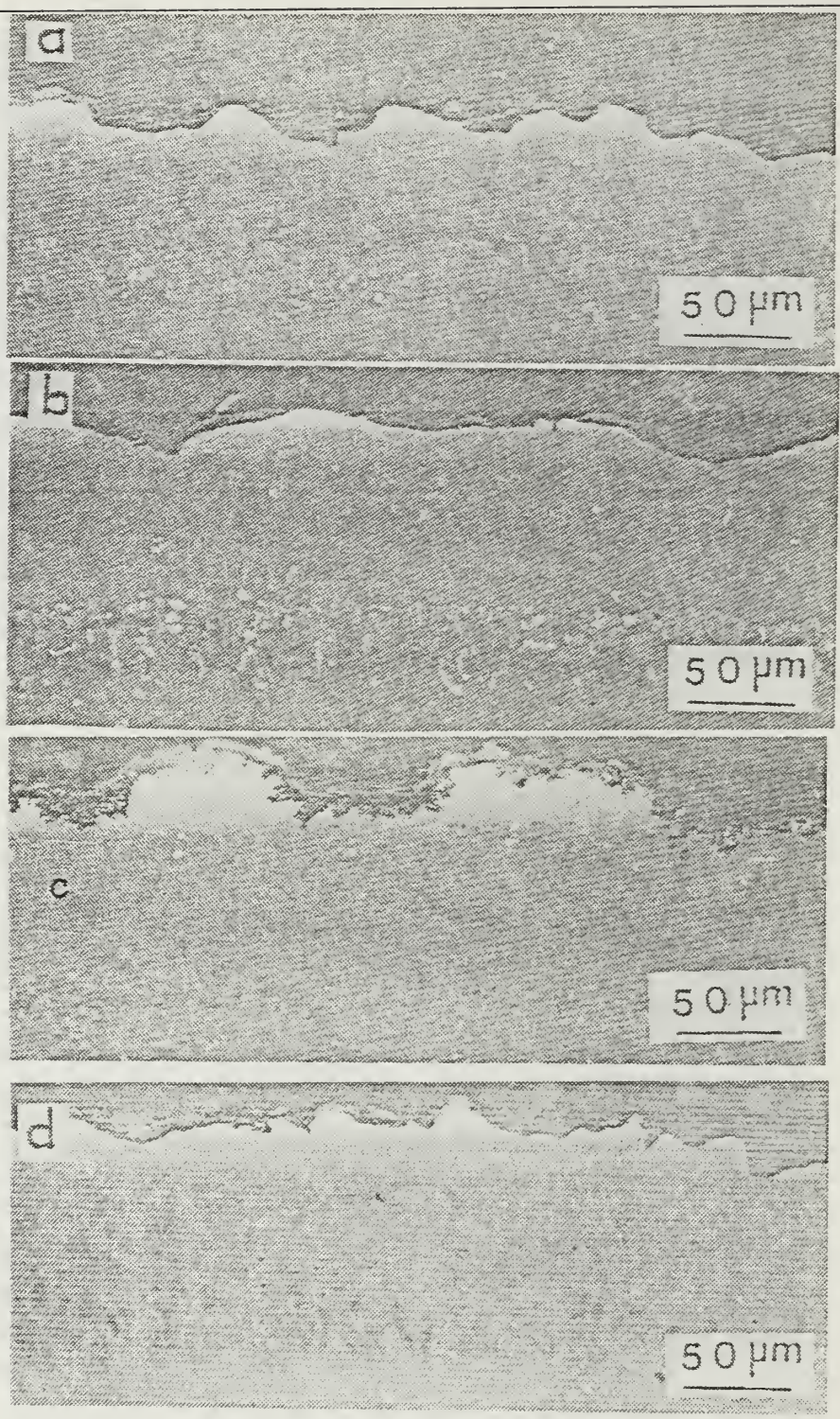

Figure B.16. Thickness Rumpling Effect for Similarly Processed Platinum Aluminide Coatings, 275 Cycles, (250 ×): a) 111Bt, b) 111BT.

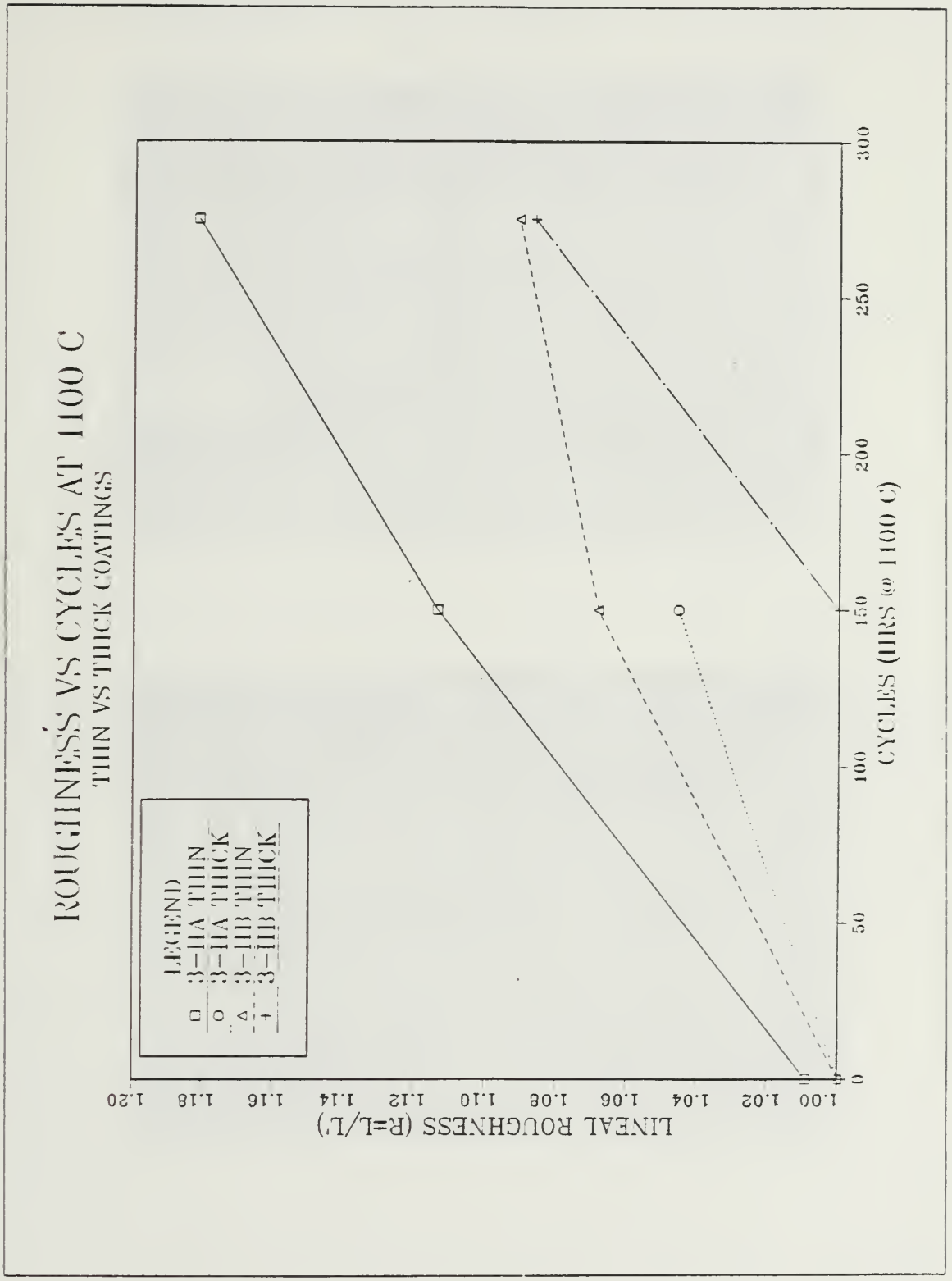

Figure B.17 Plot of Lineal Roughness versus Cyclic Exposure for a Thin and Thick Inward and Outward Platinum Aluminide Coating.

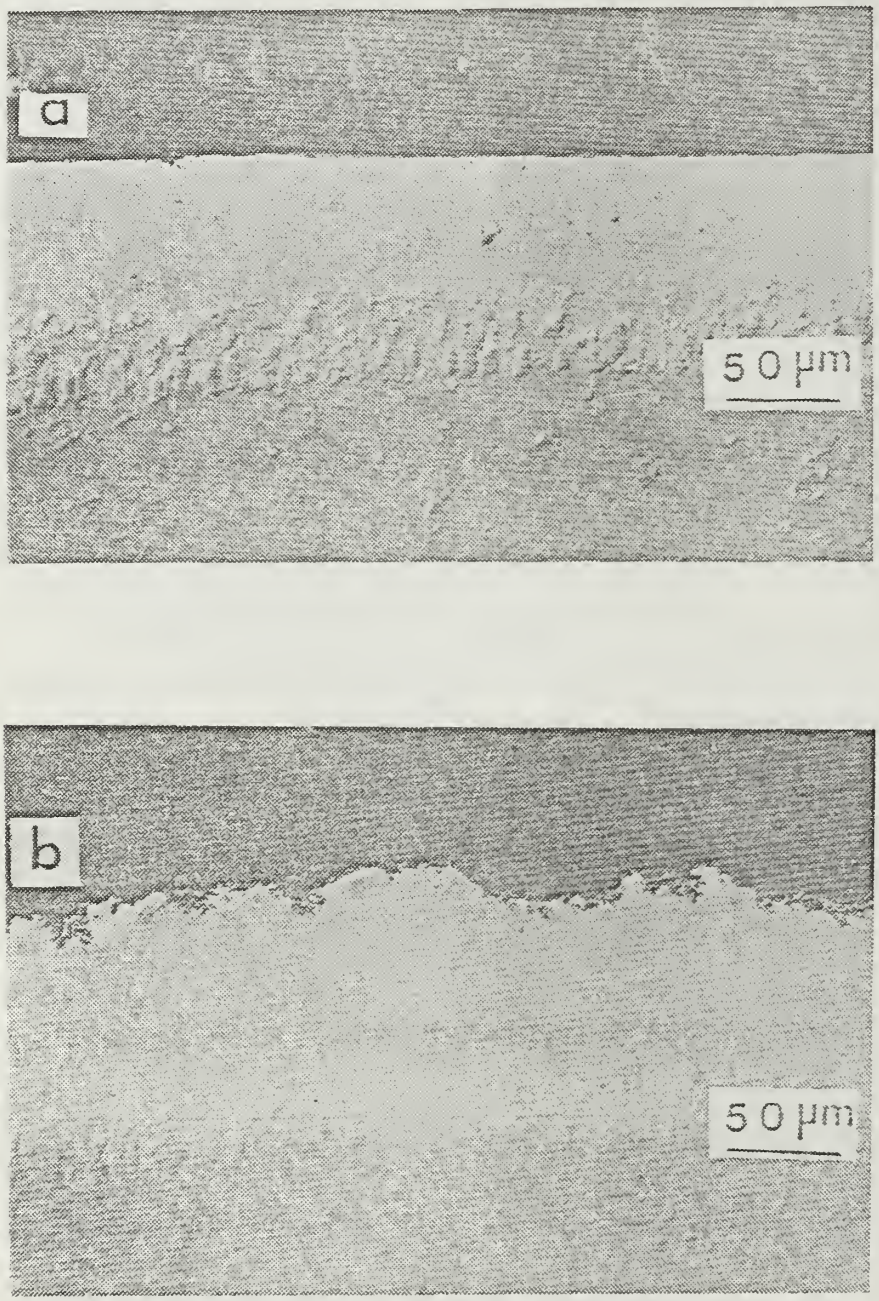

Figure B.18 Rumpling Comparison of a Thin and Thick Platinum Aluminide Coating, 150 Cycles, (250 ×): a) 3HBT, b) 3HBt.

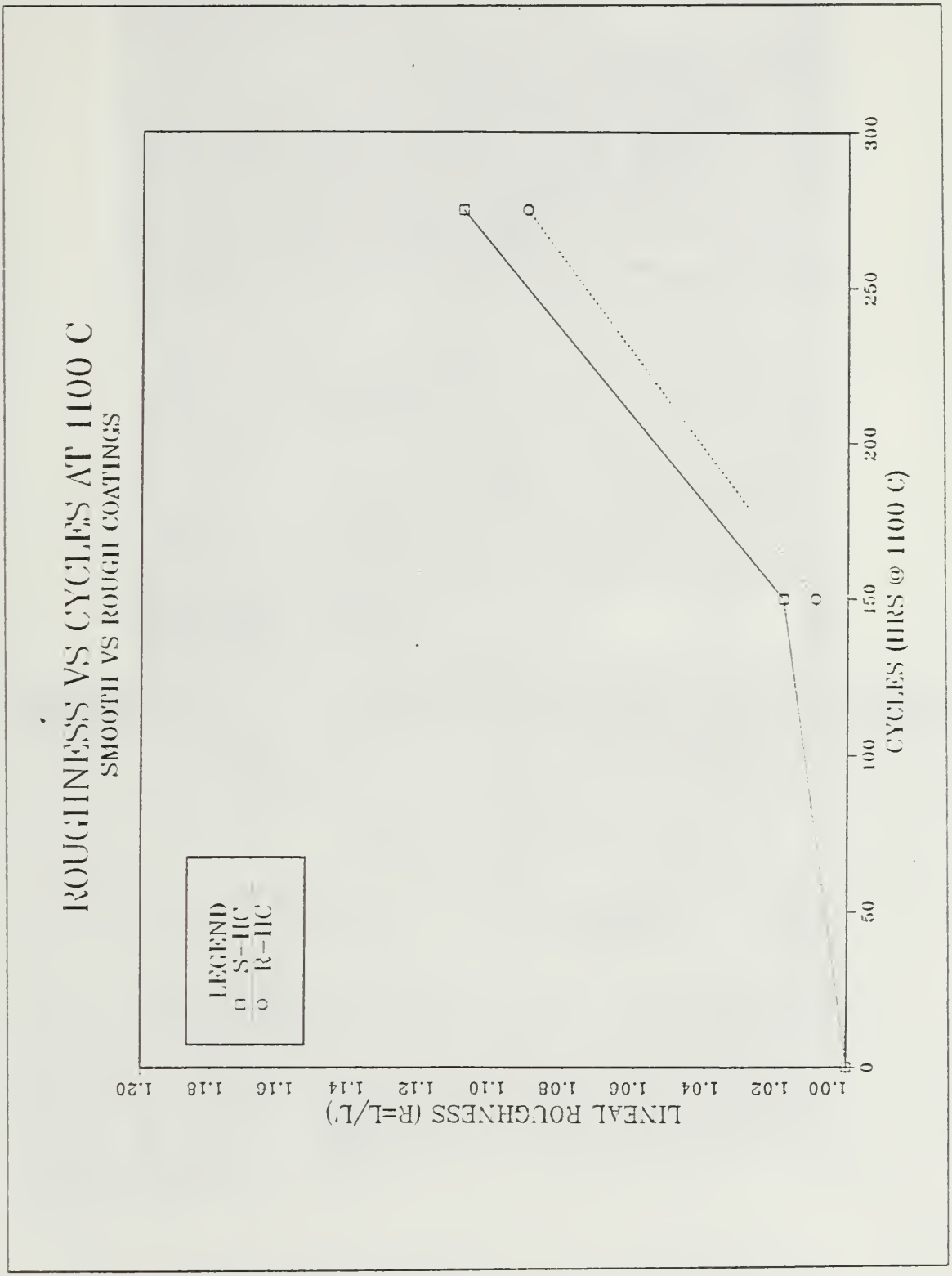

Figure B.19 Plot of Lineal Roughness versus Cyclic Exposure for Smooth and Rough Platinum Aluminide Coatings.

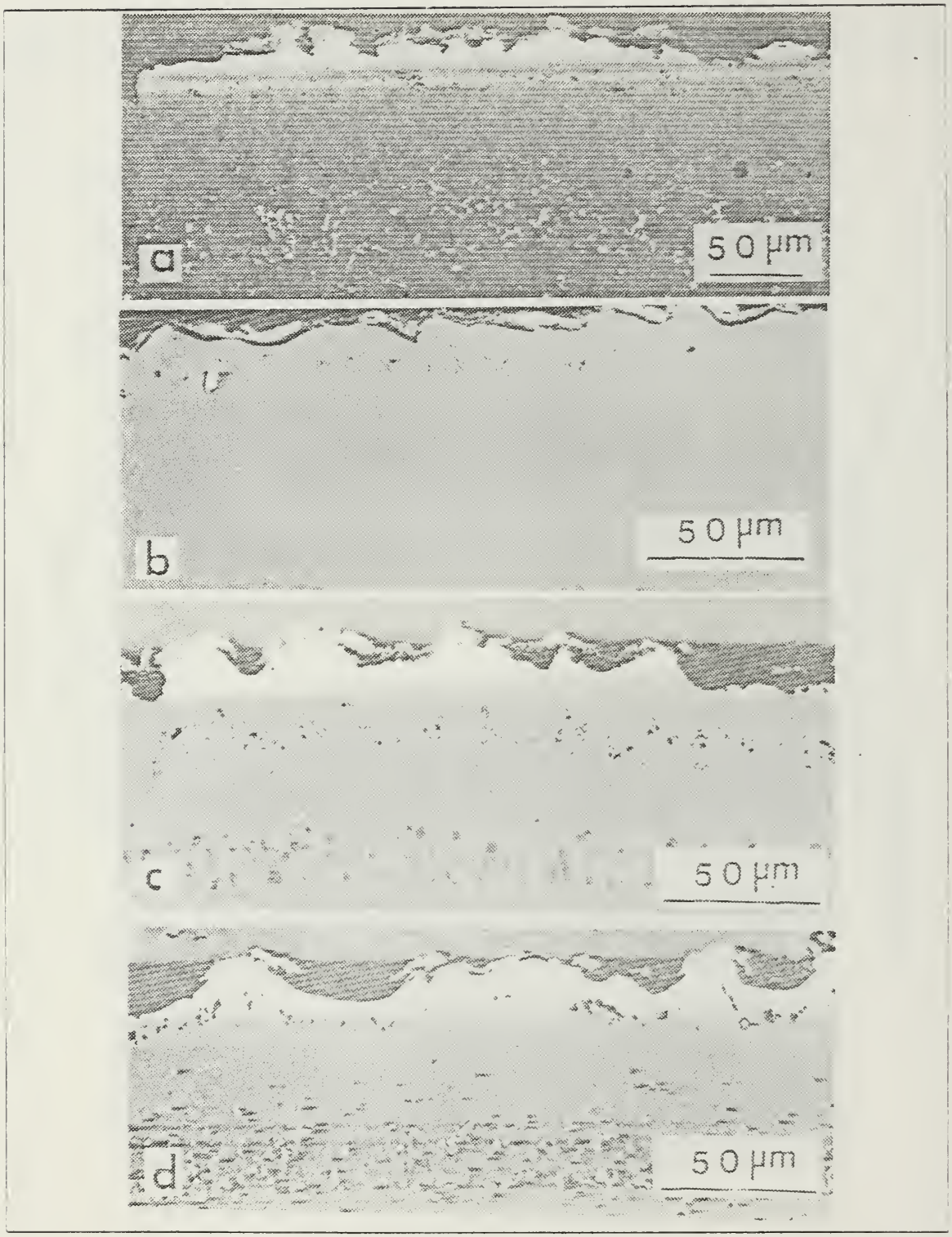

Figure B.20 Rumpling Comparisons of a Smooth and Rough Platinum Aluminide Coating, (250 ×): a) RHC, 150 cycles, b) SHC, 150 cycles, c) RHC, 275 cycles, d) SHC, 275 cycles.

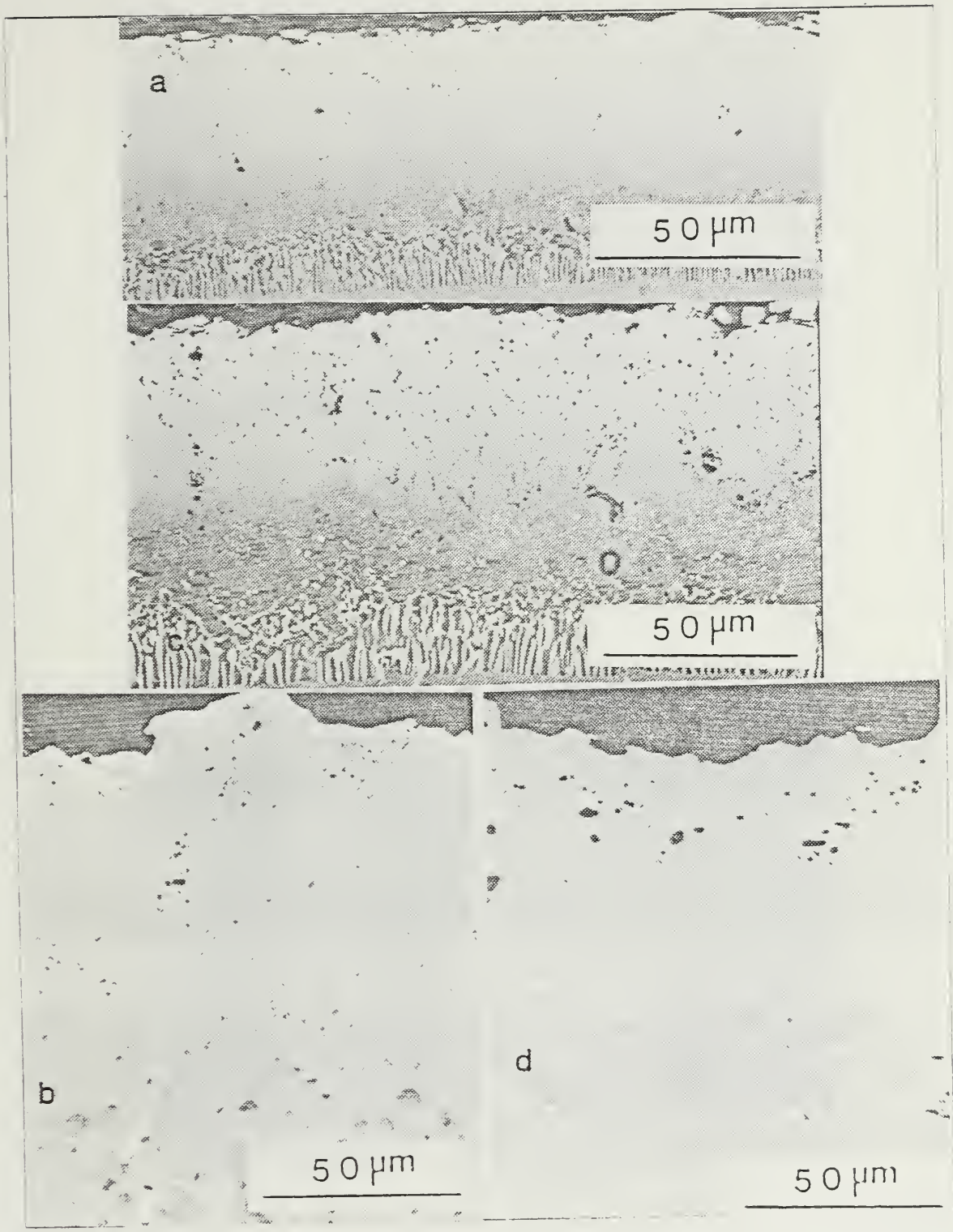

Figure B.21 Cross-section Microstructural Comparison of Initial and Thermally Cycled Platinum Aluminide Coatings. (650 ×): a) 2HAt, 0 cylces, b) 2HAt, 150 cycles, c) 3HAt, 0 cycles, d) 3HAt, 150 cycles.

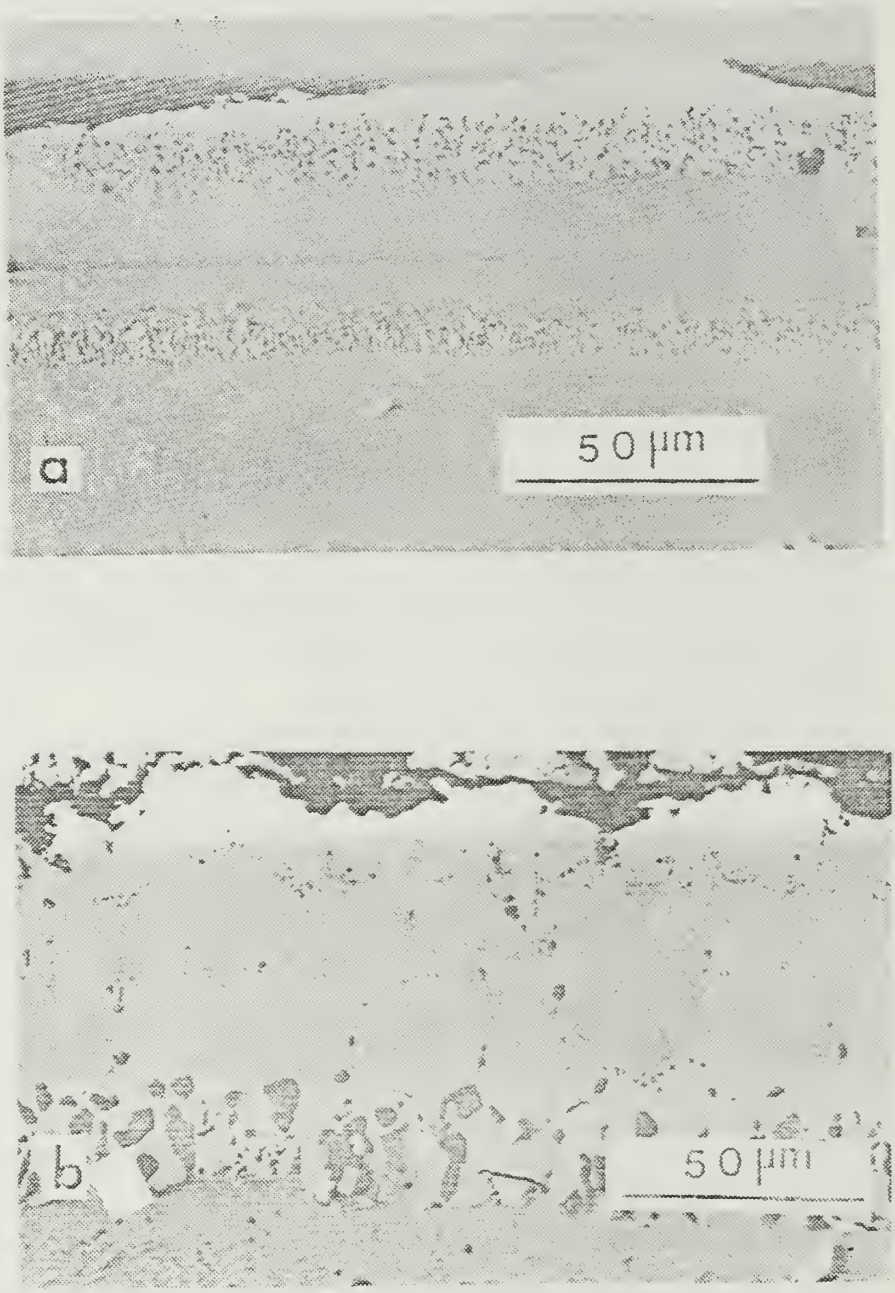

Figure B.22 Cross-section Microstructural Comparison of An Initial and Thermally Cycled Platinum Aluminide Coating, (650 ×): a) 4HAT, 0 cycles, b) 4HAT, 150 cycles.

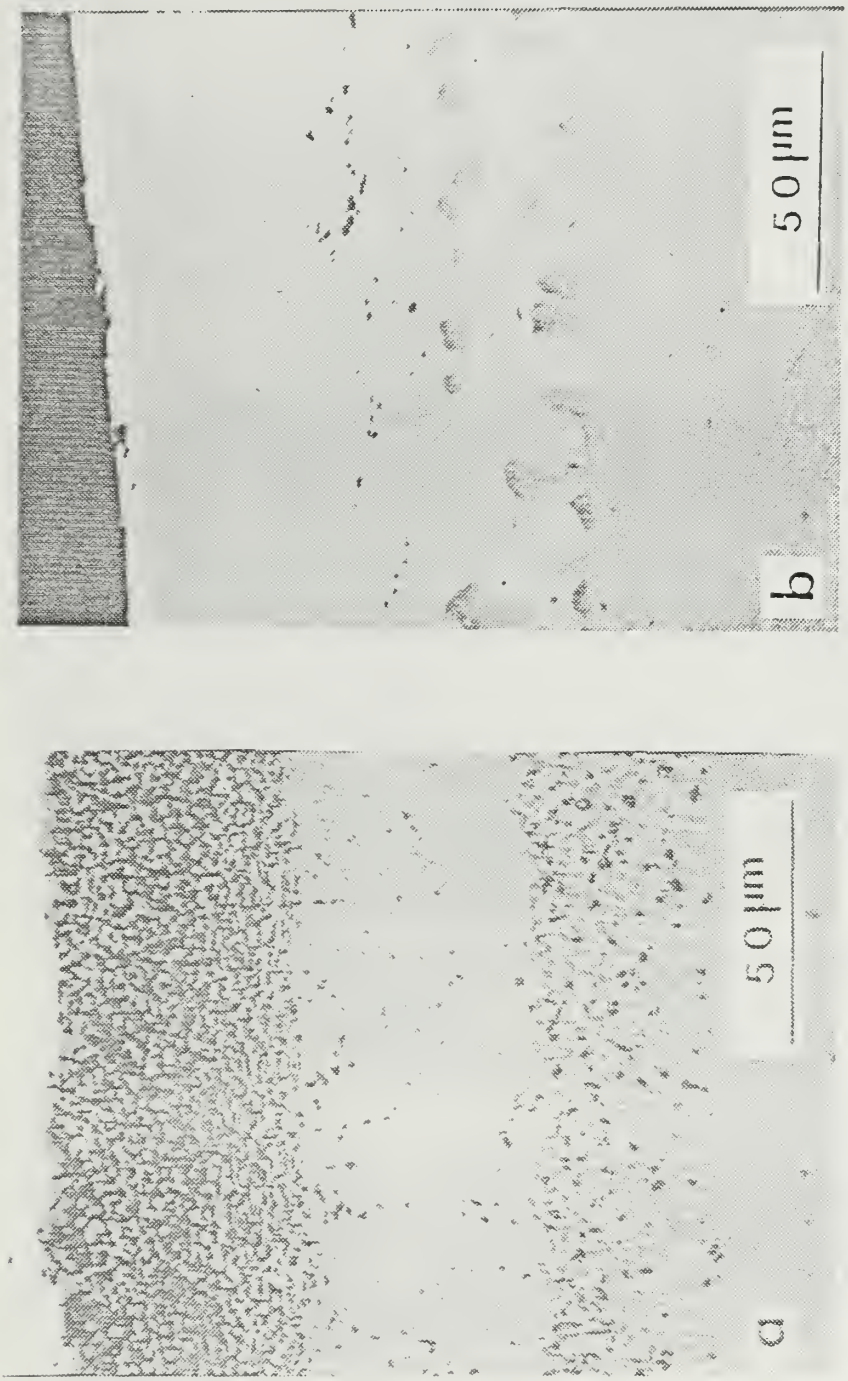

Figure B.23 Cross-section Microstructural Comparison of An Initial and Thermally Cycled Platinum Aluminide Coating, (650 ×): a) 4IIBT, 0 cycles, b) 4IIBT, 150 cycles.

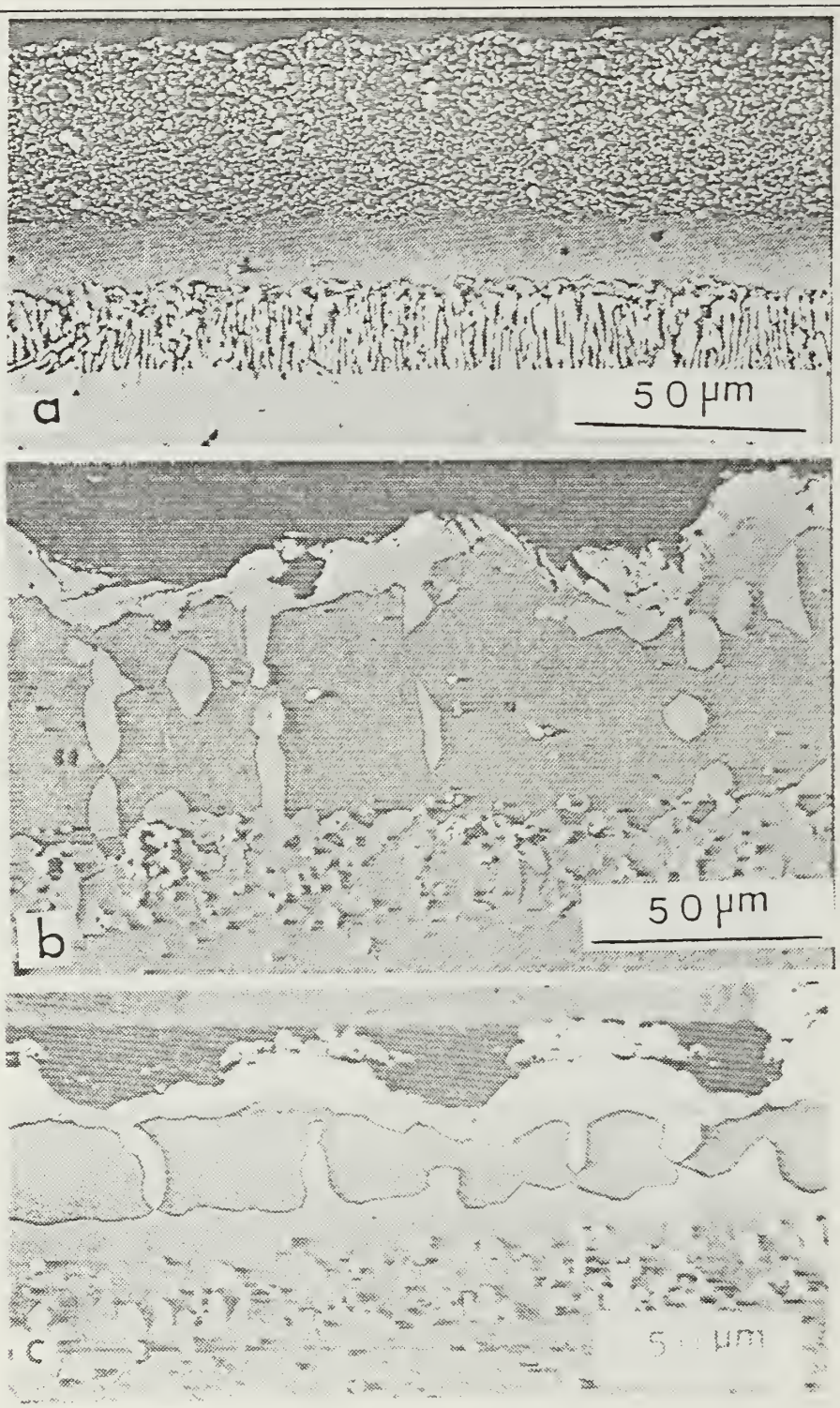

Figure B.24. Cross-section Microstructural Comparison of the Inward Baseline Coating, Initial and Thermally Cycled: a) BLA, 0 cycles (650 ×), b) BLA, 150 cycles (550 ×), c) BLA, 2~5 cycles (500 ×).

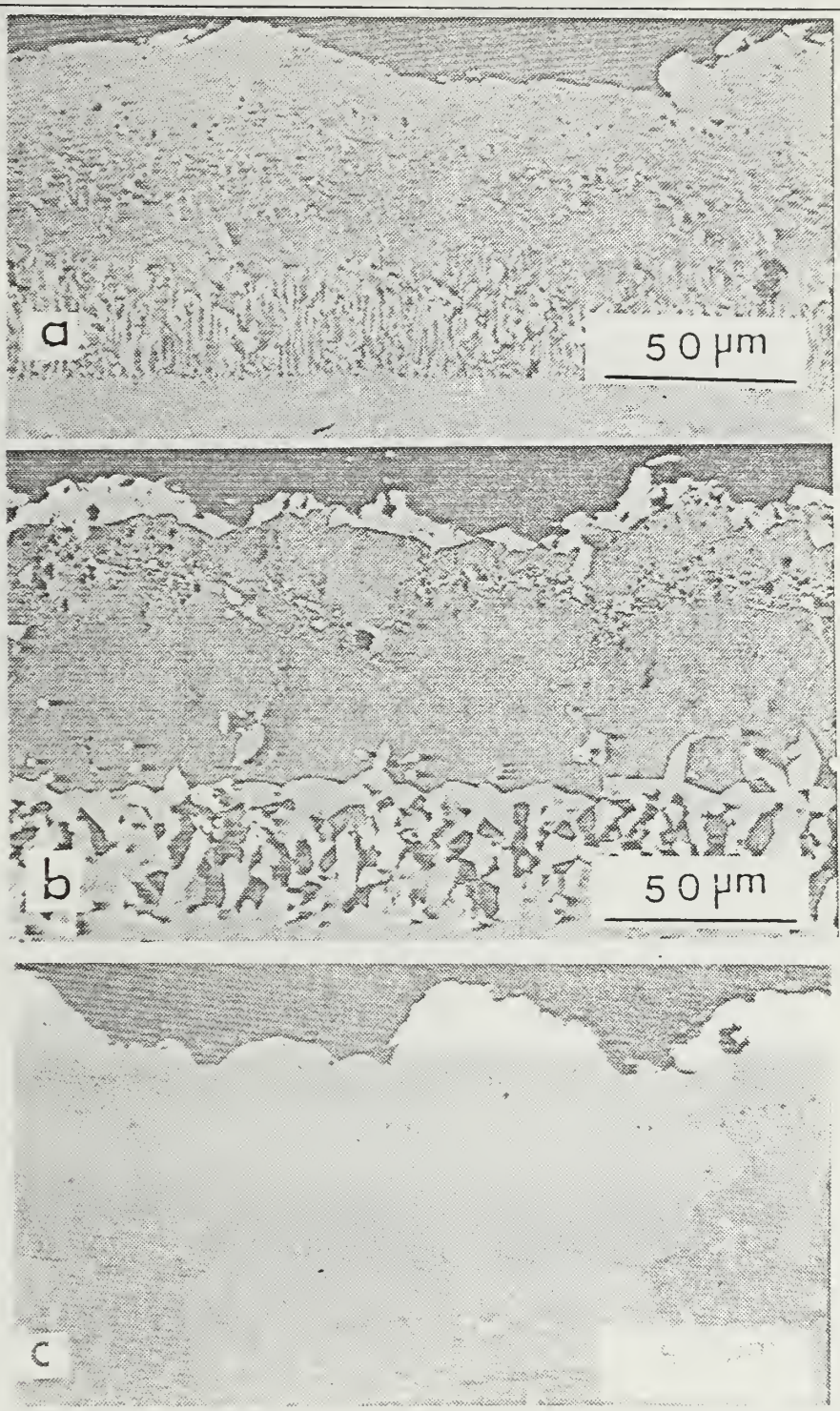

Figure B.25 Cross-section Microstructural Comparison of the Outward Baseline Coating, Initial and Thermally Cycled: a) BLB, 0 cycles (550 ×), b) BLB, 150 cycles (550 ×), c) BLB, 275 cycles (500 ×).

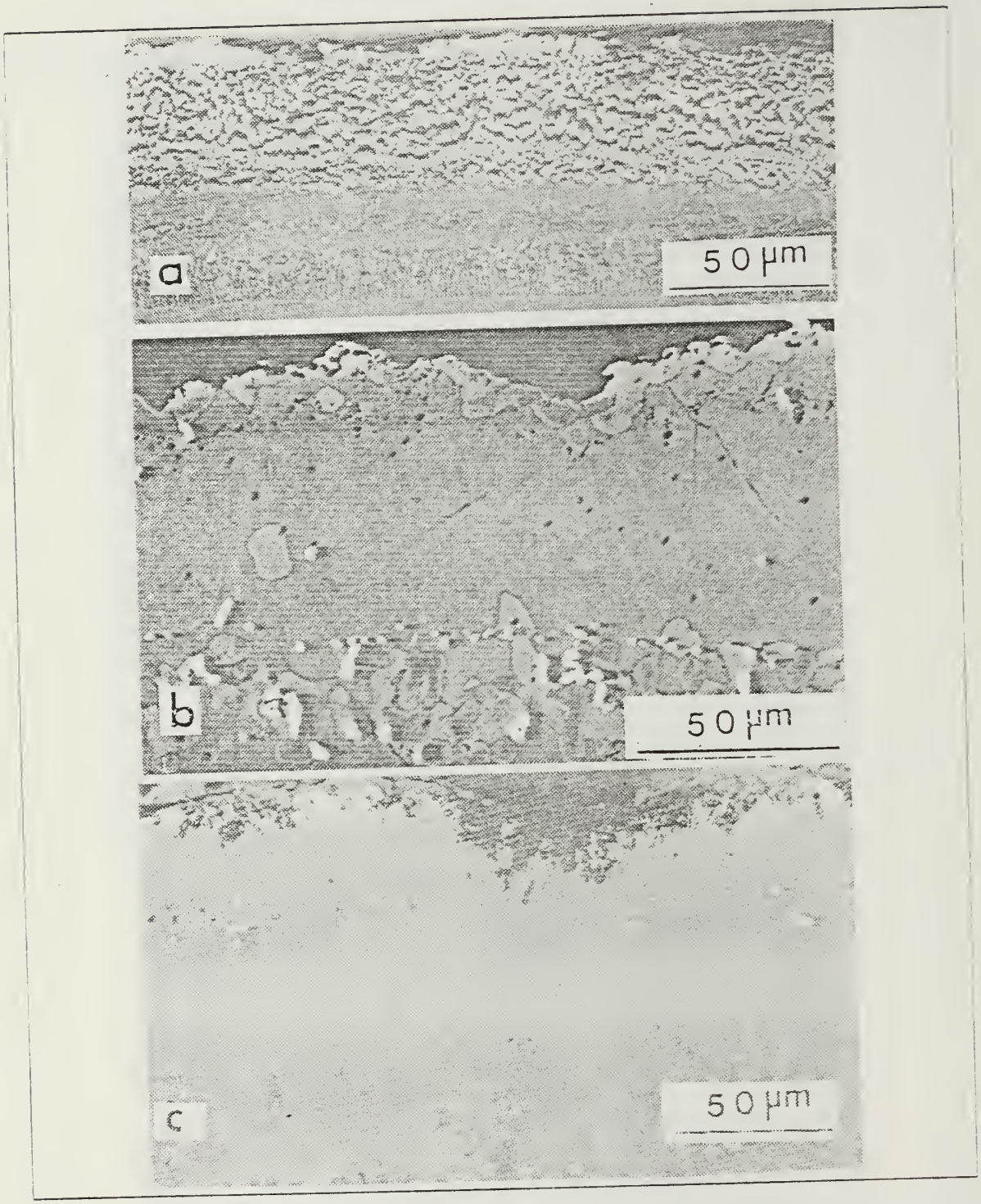

Figure B.26 Cross-section Microstructural Comparison of a Platinum Aluminide Coating, Initial and Thermally Cycled: a) 311Bt, 0 cycles (500 ×), b) 311Bt, 150 cycles (650 ×), c) 311Bt, 275 cycles (500 ×).

LIST OF REFERENCES

1. Goebel, J.A., Barkalow, R.H. and Pettit, F.S., "The Effects Produced by Platinum in High Temperature Metallic Coatings," *Proceedings of the Tri-Service Conference on Corrosion*, MCIC Report 79-40, pp. 165-185, 1979.

2. Pettit, F.S. and Goward, G.W., "High Temperature Corrosion and Use of Coatings for Protection," *Metallurgical Treatises*, AIME Conference Proceedings, Beijing, China, p. 603, 13-22 November 1981.

3. Lindblad, N.R., "A Review of the Behavior of Aluminide-Coated Superalloys," *Oxidation of Metals*, v. 4, pp. 143-170, 1969.

4. Perkins, A.J., *High Temperature Gaseous Corrosion*, Lecture notes, revised 1981.

5. Fontana, M.G., *Corrosion Engineering*, 3d ed., pp. 505-544, McGraw-Hill Book Company, Inc., 1986.

6. Pilling, N.B. and Bedworth, R.E., "Oxidation of Metals at High Temperatures," *Journal of the Institute of Metals*, v. 29, p. 529, 1923.

7. Chalmers, B., *Physical Metallurgy*, p. 445, John Wiley & Sons, Inc., 1959.

8. Shepard, S.B., "NAVSEA Marine Gas Turbine Materials Development Program," *Naval Engineers Journal*, pp. 65-75, August 1981.

9. Naval Postgraduate School Report 69-85-008, *Microstructural Formation and Effects on the Performance of Platinum Modified Aluminide Coatings*, by P. Deb and D.H. Boone, November, 1985.

10. American Society of Mechanical Engineers Report 84-GT-277, *A Long-Term Field Test of Advanced Gas Turbine Airfoil Coatings Under a Severe IndustrialEnvironment*, by K.G. Kubarych, D.H. Boone and R.L. Duncan, June 1984.

11. Goward, G.W., *Protective Coatings for High Temperature Gas Turbine Alloys: A Review of the State of Technology*, paper presented at the NATO Advanced Study Institute on Surface Engineering, Les Arcs, France, 13-15 July 1983.

12. Nicoll, A.R., *A Survey of Methods Used for the Performance Evaluations of High Temperature Coatings*, paper presented at the Coatings for High Temperature Applications Seminar, Petten, Holland, 8-11 March 1982.

13. Restall, J.E., "High Temperature Coatings for Protecting Hot Components in Gas Turbine Engines," *Metallurgia*, November 1979.

14. Scelig, R.P. and Stueber, R.J., "High-Temperature-Resistant Coatings for Superalloys," *High Temperatures--High Pressures*, v. 10, 1978.

15. Goward, G.W., Boone, D.H., and Giggins, C.S., "Formation and Degradation Mechanisms of Aluminide Coatings on Nickel-Base Superalloys," *ASM Trans. Quart.*, v.60, 1967.

16. Hancock, P., Hurst, R.C., and Wysiekierski, A.G., "The Influence of Thermal Cycling and Surface Degradation on Hot Corrsion," *Proceedings of the Third Conference on Gas Turbine Materials in a Marine Enviroment*, Bath, U.K., Session V, Paper 3, 1976.

17. Smialek, J.L., "Oxide Morphology and Spalling Model for NiAl," *Metallurgical Transactions*, v. 9A, pp. 309-320, 1978.

18. Materials Research Laboratories, Department of Defense, Australia, Report MRL-R-280, *Diffusion Aluminide Coatings*, by G.R. Johnston and P.G. Richards, Unclassified, May 1981.

19. Lehnert, G. and Meinhardt, H.W., "A New Protective Coating for Nickel Alloys," *Electrodeposition and Surface Treatments*, v. 1, pp. 189-197, 1972/3.

20. Lehnert, G. and Meinhardt, H.W., "Present State and Trend of Development of Surface Coating Methods Against Oxidation and Corrosion at High Temperatures," *Electrodeposition and Surface Treatments*, v. 1, pp.71-76, 1972/3.

21. Streiff, R., Boone, D.H., and Purvis, L.J., *Structure of Platinum Modified Aluminide Coatings*, paper presented at the NATO Advanced Study Institute on Surface Engineering, Les Arcs, France, 13-15 July 1983.

22. Manley, T.F., *Plastic Instabiltiy of Aluminide and Platinum Modified Diffusion Coatings During 1100°C Cyclic Testing* Master's Thesis, Naval Postgraduate School, Monterey, California, December, 1985.

23. Deb, P., Boone, D.H., and Manley, T.F., "Surface Instability of Platinum Modified Aluminide Coatings During 1100°C Cyclic Testing," *Proceedings of the 13th International Conference on Metallurgical Coatings*, San Diego, California, April, 1986.

24. Strangman, T.E., *Thermal Fatigue of Oxidation Resistant Overlay Coatings for Superalloys*, Ph.D. Dissertation, University of Connecticut, 1978.

25. Mevrel, R., *Cyclic Oxidation of High Temperature Alloys*, paper presented at the High Temperature Corrosion of Superalloys Symposium, London, England, 11-12 February 1986.

26. Vogel, D.J., *Determination of the Ductile to Brittle Transition Temperature of Platinum-Aluminde Gas Turbine Blade Coatings*, Master's Thesis, Naval Postgraduate School, Monterey, California, September, 1985.

27. Douglas, D.L., "Exfoliation and the Mechanical Behavior of Scales," *Oxidation of Metals and Alloys*, American Society for Metals, Metals Park, Ohio, pp. 137-156, 1971.

28. Lowell, C.E., Smialak, J.L., and Barrett, C.A., "Cyclic Oxidation of Superalloys," *High Temperature Corrosion*, pp. 219-226, NACE, 1983.

29. Air Force Materials Laboratory Report AFW-TR-83-4086, *Advanced Coating Research and Development*, by R.H. Barkalow, R.J. Hecht and R.E. Shamakian, p. 39, February 1985.

30. McCall, J.L. and Steele, J.H., Jr., *Practical Applications of Quantitative Metallography*, ASTM Special Technical Publication 839, p. 171, 1983.

31. Newman, L.G., *Structural Property Effects for Platinum Modified Aluminide Coatings*, Master's Thesis, Naval Postgraduate School, Monterey, California, September 1986.

32. Farrell, M.S., *An Investigation of the Oxide Adhesion and Growth Characteristics on Platinum Modified Aluminide Coatings*, Master's Thesis, Naval Postgraduate School, Monterey, California, September 1986.

INITIAL DISTRIBUTION LIST

		No. Copies
1.	Defense Technical Information Center Cameron Station Alexandria, Virginia 22304-6145	2
2.	Library Code 0142 Naval Postgraduate School Monterey, California 93943-5002	2
3.	Mr. William Barker Naval Air Development Center Code 60634 Warminster, Pennsylvania 18974-5000	1
4.	Department Chairman, Code 69M Department of Mechanical Engineering Naval Postgraduate School Monterey, California 93943-5000	1
5.	Adjunct Professor D.H. Boone, Code 69B Department of Mechanical Engineering Naval Postgraduate School Monterey, California 93943-5000	5
6.	Commander, Naval Air Systems Command Department of the Navy (803) Washington, D.C. 20361	1
7.	LT M.A. McCloskey 7409 Glencagles Road Norfolk, Virginia 23505	2

220796

Thesis
M17545 McCloskey
c.1 Plastic instability of platinum modified and unmodified aluminide coatings during 1100 C cyclic testing.